SAT1000

Searching for footprints of saturation in proton-proton collisions

Antoni Szczurek [1,2]
Anna Cisek [2]
Wolfgang Schäfer [1]

[1]Institute of Nuclear Physics PAN Kraków
[2]University of Rzeszów

Introduction

- Did we already see (onset of) saturation ?
  - Low-x, low-Q^2 DIS (GBW and many others)
    There are alternative approaches.
  - High-energy, low-p_t particle production (McLarran-Praszalowicz)
  - pA processes.
- Where to search for saturation effects ?

Contents

Literature

The presented work is based on our recent analyses:

W. Schäfer and A. S.,
“Low mass Drell-Yan production of lepton pairs at forward directions at the LHC: A hybrid approach”, arXiv:1602.06740, Phys. Rev. **D93** (2016) 074014.

A. Cisek, W. Schäfer and A. Szczurek, “Exclusive photoproduction of charmonia in $\gamma p \to Vp$ and $pp \to pVp$ reactions within k_t-factorization approach”,
JHEP **1504** (2015) 159. Phys. Rev. **D93** (2016) 074014.

A. Cisek, W. Schäfer and A. S., "Semiexclusive production of J/ψ mesons in proton-proton collisions", arXiv:1611.08210.

A. Cisek and A. S., a paper in preparation

Drell-Yan at low dilepton invariant masses

Where the dipole formulae apply ?
Do we observe a sign of saturation ?

Introduction to Drell-Yan

1. The Drell-Yan process is one of important sources of the partonic structure
2. Drell-Yan production of low invariant masses in forward direction could be a good place in searching for onset of (gluon) saturation because small-x region
   (Brodsky et al., Gelis and Jalilian-Marian, ...)
3. Color dipole model with parametrized dipole-nucleon cross section in the so-called mixed representation inspired by saturation is often used.
   Only some observables available,
   not full kinematics, no experimental cuts on individual kinematical variables of leptons available
4. k_t-factorization with unintegrated quark/antiquark distribution functions (Szczurek-Slipek, Nefedov-Nikolaev-Saleev, Baranov-Lipatov-Zotov) was also used at mid rapidities.
5. At forward/backward directions (low-x) gluon distributions have to be taken into account (formally higher order).
6. A hybrid (collinear, k_t-factorization) approach is proposed, using UGDFs, with control of momenta of individual leptons

Dipole approach to the Drell-Yan process

- Brodsky, Hebecker, Quack, Phys. Rev. D55, 2584 (1997)
- Kopeliovich, Tarasov, Schäfer, Phys. Rev. C59, 1609 (1999)
- Betemps, Ducati, Machado, Phys. Rev. D66 014018 (2002)
- Betemps, Ducati, Machado, Raufeisen, Phys. Rev. D67 114008 (2003)
- Golec-Biernat, Lewandowska, Stasto, Phys. Rev. D82, 094010 (2010)
- Ducati, Griep, Machado, Phys. Rev. D66, 094014 (2014)
- Motyka, Sadzikowski, Stebel, JHEP 05, 087 (2015) (twist expansion and agular distributions)
- Basso, Goncalves, Nemchik, Pasechnik, Sumbera, Phys. Rev. D93, 034023 (2016) (also for Z boson production)

Short personal summary and critical remarks

- All in the so-called mixed (transverse position space) representation, use saturation inspired parametrizations of dipole-nucleon cross section.
- Approximate kinematics - only variables of the diphoton explicit (α and $p_{t,pair}$), associated jet not included in calculating x.
- Only one-side contribution included
- Not sufficient when cuts on individual leptons required.
- So far applied to rather low energies and midrapidities where the formalism does not apply.

Forward and backward production of dilepton pairs

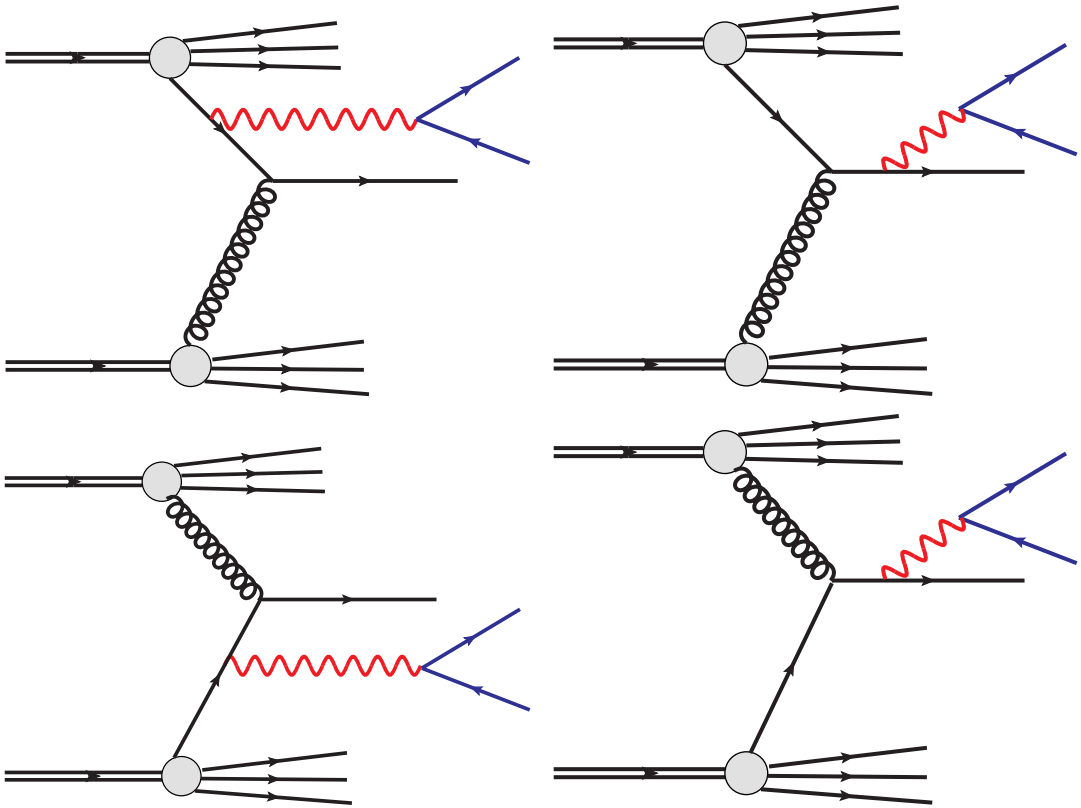

Figure: The diagrams relevant for forward and backward production of dilepton pairs.

Similar diagrams as in the dipole approach.

k_T-factorization form

The full dilepton cross section is then

$$
\begin{aligned}
\frac{d\sigma(pp \to l^+l^-X)}{dy_+dy_-d^2\boldsymbol{k}_+d^2\boldsymbol{k}_-} &= x_+x_-\frac{d\sigma(pp \to l^+l^-X)}{dx_+dx_-d^2\boldsymbol{k}_+d^2\boldsymbol{k}_-} \\
&= \frac{\alpha_{\rm em}^2}{8\pi^2 N_c M^2}\sum_f e_f^2 \int_{x_F}^1 dx_1 \left[x_1 q_f(x_1,\mu^2) + x_1\bar{q}_f(x_1,\mu^2)\right] \\
&\quad \int \frac{d^2\boldsymbol{\kappa}_2}{\pi\boldsymbol{\kappa}_2^4}\mathcal{F}(x_2,\boldsymbol{\kappa}_2^2)\alpha_S(\bar{q}^2) \\
&\quad \Big\{\frac{x_F}{x_1}I_T\left(\frac{x_F}{x_1},\boldsymbol{q},\boldsymbol{\kappa}_2\right)D_T\left(\frac{x_+}{x_F}\right) \\
&\quad +\frac{x_F}{x_1}I_L\left(\frac{x_F}{x_1},\boldsymbol{q},\boldsymbol{\kappa}_2\right)D_L\left(\frac{x_+}{x_F}\right) \\
&\quad +\frac{x_F}{x_1}I_\Delta\left(\frac{x_F}{x_1},\boldsymbol{q},\boldsymbol{\kappa}_2\right)D_\Delta\left(\frac{x_+}{x_F}\right)\left(\frac{\boldsymbol{l}}{|\boldsymbol{l}|}\cdot\frac{\boldsymbol{q}}{|\boldsymbol{q}|}\right) \\
&\quad +\frac{x_F}{x_1}I_{\Delta\Delta}\left(\frac{x_F}{x_1},\boldsymbol{q},\boldsymbol{\kappa}_2\right)D_{\Delta\Delta}\left(\frac{x_+}{x_F}\right)\left(2\left(\frac{\boldsymbol{l}}{|\boldsymbol{l}|}\cdot\frac{\boldsymbol{q}}{|\boldsymbol{q}|}\right)^2-1\right)\Big\}\,.
\end{aligned}
$$

k_T-factorization form

If we also want to include the recoiling jet - insert

$$dx_J \delta(x_J + x_F - x_1)\, d^2\boldsymbol{k}_J\, \delta^{(2)}(\boldsymbol{\kappa}_2 - \boldsymbol{q} - \boldsymbol{k}_J)\,. \tag{1}$$

This gives us the fully differential distribution

$$\begin{aligned}
\frac{d\sigma(pp \to l^+ l^- X)}{dy_+ dy_- dy_J d^2\boldsymbol{k}_+ d^2\boldsymbol{k}_- d^2\boldsymbol{k}_J} \quad = \quad & \frac{\alpha_{\rm em}^2}{8\pi^3 N_c M^2} \frac{x_F x_J}{x_F + x_J} \\
& \times \sum_f e_f^2 \left[q_f(x_F + x_J, \mu^2) + \bar{q}_f(x_F + x_J, \mu^2) \right] \\
& \frac{\alpha_S(\bar{q}^2) \mathcal{F}(x_2, \boldsymbol{q} + \boldsymbol{k}_J)}{(\boldsymbol{q} + \boldsymbol{k}_J)^4} \\
& \times \Big\{ I_T^f \Big(\frac{x_F}{x_F + x_J}, \boldsymbol{q}, \boldsymbol{q} + \boldsymbol{k}_J \Big) D_T \Big(\frac{x_+}{x_F} \Big) \\
+ \quad & I_L^f \Big(\frac{x_F}{x_F + x_J}, \boldsymbol{q}, \boldsymbol{q} + \boldsymbol{k}_J \Big) D_L \Big(\frac{x_+}{x_F} \Big) \\
+ \quad & I_\Delta^f \Big(\frac{x_F}{x_F + x_J}, \boldsymbol{q}, \boldsymbol{q} + \boldsymbol{k}_J \Big) D_\Delta \Big(\frac{x_+}{x_F} \Big) \Big(\frac{\boldsymbol{l}}{|\boldsymbol{l}|} \cdot \frac{\boldsymbol{q}}{|\boldsymbol{q}|} \Big) \\
+ \quad & I_{\Delta\Delta}^f \Big(\frac{x_F}{x_F + x_J}, \boldsymbol{q}, \boldsymbol{q} + \boldsymbol{k}_J \Big) D_{\Delta\Delta} \Big(\frac{x_+}{x_F} \Big) \Big[2 \Big(\frac{\boldsymbol{l}}{|\boldsymbol{l}|} \cdot \frac{\boldsymbol{q}}{|\boldsymbol{q}|} \Big)^2 - 1 \Big] \Big\}\,.
\end{aligned} \tag{2}$$

Kinematics

Rapidities are obtained as:

$$y_i = \log\left(\frac{x_i\sqrt{S}}{\sqrt{\boldsymbol{k}_i^2}}\right) \leftrightarrow x_i = \sqrt{\frac{\boldsymbol{k}_i^2}{S}} \cdot e^{y_i}\,, i = +, -, J\,. \tag{3}$$

The longitudinal momentum fractions x_1, x_2 entering the quark and gluon distributions are

$$\begin{aligned} x_1 &= \sqrt{\frac{\boldsymbol{k}_+^2}{S}}e^{y_+} + \sqrt{\frac{\boldsymbol{k}_-^2}{S}}e^{y_-} + \sqrt{\frac{\boldsymbol{k}_J^2}{S}}e^{y_J}\,, \\ x_2 &= \sqrt{\frac{\boldsymbol{k}_+^2}{S}}e^{-y_+} + \sqrt{\frac{\boldsymbol{k}_-^2}{S}}e^{-y_-} + \sqrt{\frac{\boldsymbol{k}_J^2}{S}}e^{-y_J}\,. \end{aligned} \tag{4}$$

The invariant mass of the dilepton system is

$$M^2 = m_{\perp+}^2 + m_{\perp-}^2 + 2m_{\perp+}m_{\perp-}\cosh(y_+ - y_-) - \boldsymbol{q}^2\,,\ \ m_{\perp\pm} = \sqrt{\boldsymbol{k}_\pm^2 + m_\pm^2}\,. \quad ($$

Fourier transform of dipole - nucleon cross section

The dipole cross section is related to the unintegrated glue as

$$\sigma(x,\boldsymbol{r}) = \frac{4\pi}{N_c}\int \frac{d^2\boldsymbol{\kappa}}{\boldsymbol{\kappa}^4}\alpha_S\mathcal{F}(x,\boldsymbol{\kappa})\Big\{1-\exp(i\boldsymbol{\kappa}\boldsymbol{r})\Big\}\,. \tag{6}$$

The parametrizations of Albacete et al. are presented in the form

$$\sigma(x,\boldsymbol{r}) = \sigma_0\cdot N(x,\boldsymbol{r})\,, \tag{7}$$

with $N(x,\boldsymbol{r})\to 1$ at large $\boldsymbol{r}$. We can therefore easily obtain, that

$$\frac{\alpha_S\mathcal{F}(x,\boldsymbol{\kappa})}{\boldsymbol{\kappa}^4} = \frac{\sigma_0 N_c}{4\pi}\int\frac{d^2\boldsymbol{r}}{(2\pi)^2}\exp(-i\boldsymbol{\kappa}\boldsymbol{r})\Big[1-N(x,\boldsymbol{r})\Big]\,, \tag{8}$$

or

$$\mathcal{F}(x,\boldsymbol{\kappa}) = \frac{\sigma_0 N_c}{8\pi^2}\frac{\boldsymbol{\kappa}^2}{\alpha_S(\boldsymbol{\kappa}^2)}\int_0^\infty rdrJ_0(\kappa r)\Big[1-N(x,\boldsymbol{r})\Big], \tag{9}$$

where $J_0(x)$ is the Bessel function. The Fourier-Bessel (or Hankel-) transform (9) can pose severe numerical problems, if values at large $\boldsymbol{\kappa}^2$ are required. For the evaluations of these integrals we use therefore a dedicated code FFTLog.

UGDFs used

We use the following UGDFs:

- Kimber-Martin-Ryskin UGDF,
  transverse momentum in the last step of evolution
- Kutak-Staśto UGDF,
  includes nonlinear effects
- Albacete, Armesto, Milhano, Salgado
  - solving BK evolution equation and Fourier transform.
- Golec-Biernat UGDF,
  saturation inspired parametrization of photon-nucleon cross section.

Parton distributions

In the present calculations we use MSTW08 distributions to generate the KMR unintegrated gluon distributions. Here we use numerical implementation by Maciuła and Szczurek used e.g. in the production of charm and double charm.
For the quark and antiquark distributions we use MSTW08 leading-order distributions. For most of the calculations we used M_{ll}^2 both as a factorization and renormalization scales. We have also tried:

$$\begin{aligned} \mu_R^2 &= \max\left(\kappa_\perp^2, q_\perp^2 + \varepsilon^2\right) , \\ \mu_F^2 &= q_\perp^2 + \varepsilon^2 . \end{aligned} \tag{10}$$

The corresponding results turned out to be almost identical.

Full rapidity range

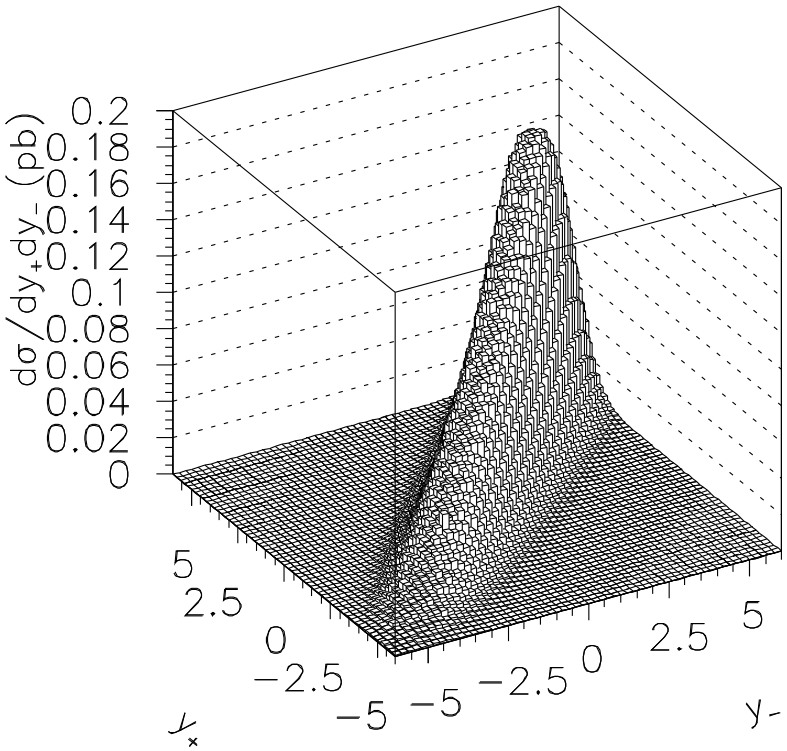

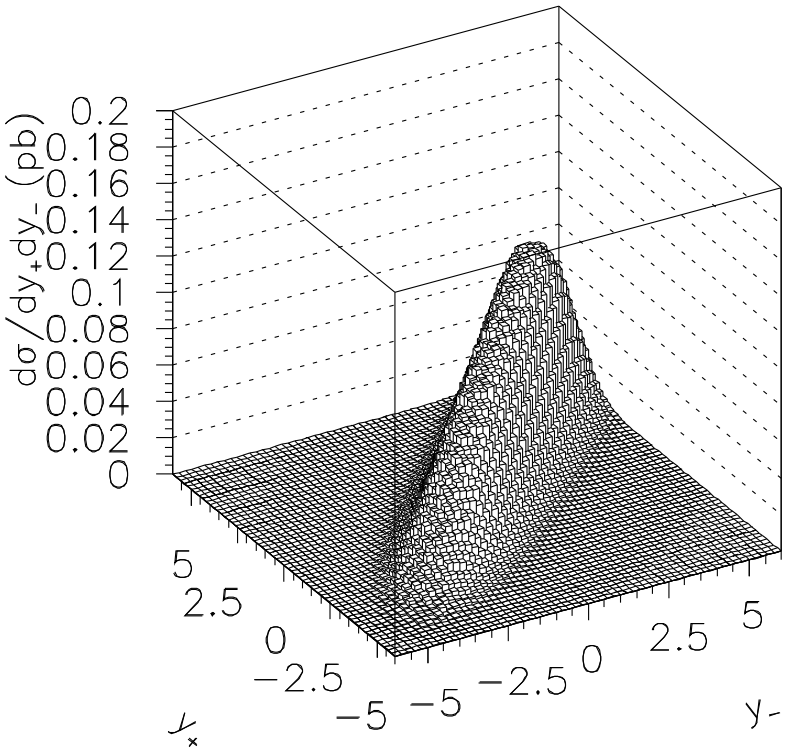

Figure: Two-dimensional (y_+, y_-) distribution for $\sqrt{s}$ = 7 TeV and $k_{T+}, k_{T-} >$ 3 GeV for MSTW08 PDF and KMR (left) and KS (right) UGDFs.

The rapidities of both leptons are strongly correlated i.e. $y_+ \approx y_-$.

Full rapidity range

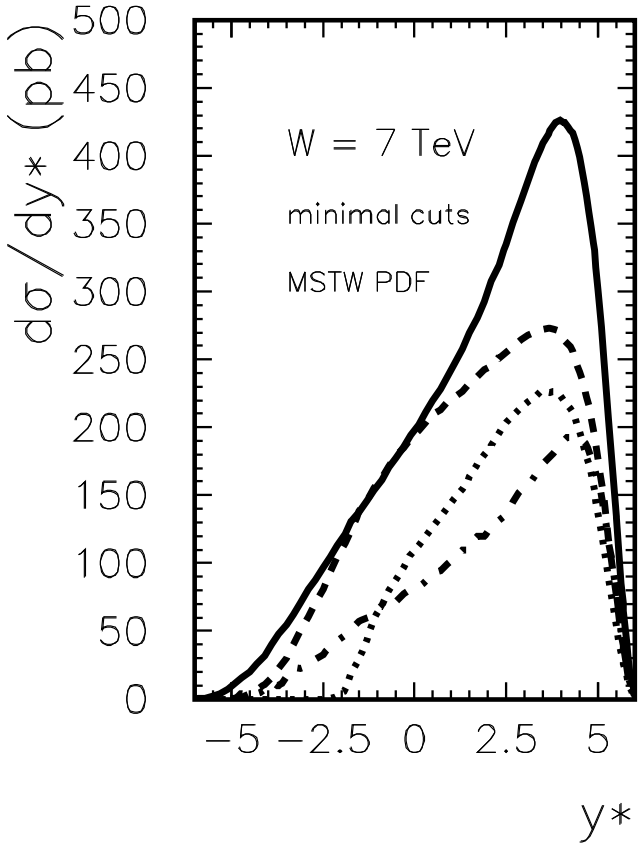

Figure: Distribution in rapidity of the dileptons for $\sqrt{s}$ = 7 TeV and $k_{T+}, k_{T-} >$ 3 GeV for MSTW08 PDF and different UGDFs: KMR (solid), KS (dashed), AAMS (dotted) and GBW (dash-dotted).

Full rapidity range

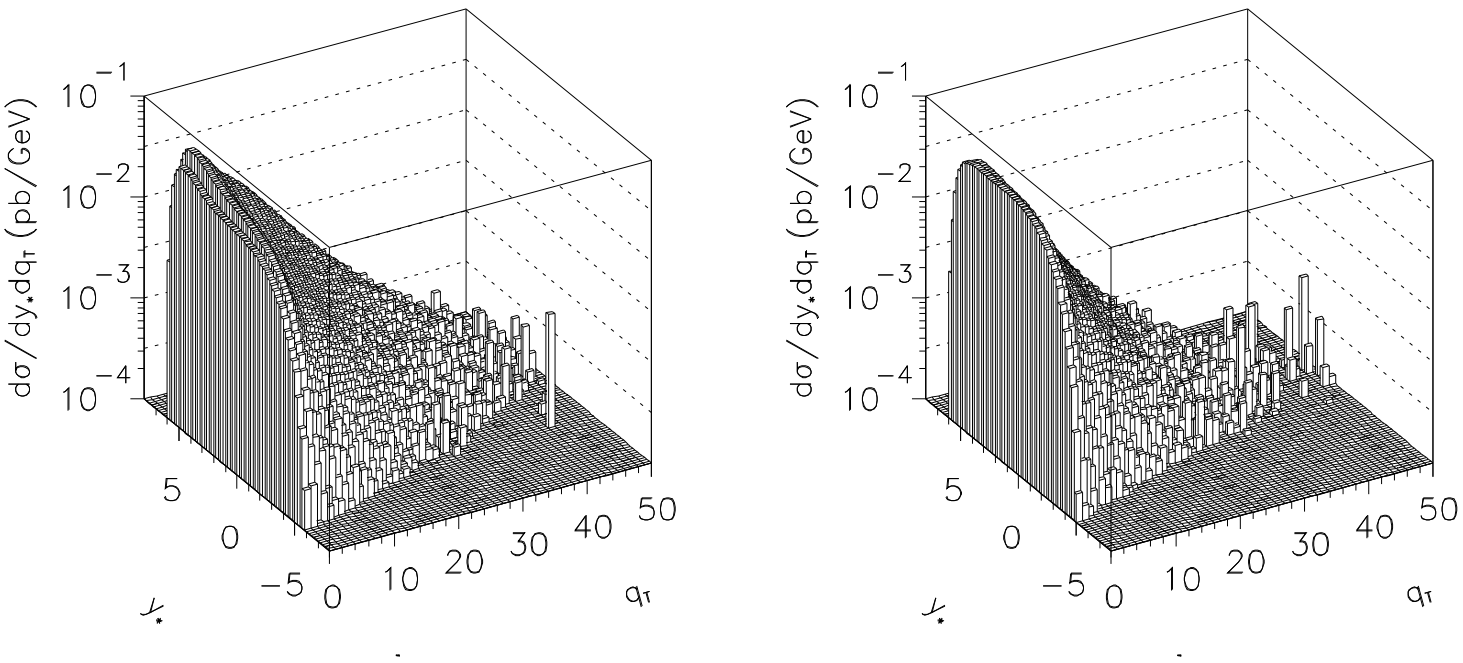

Figure: Two-dimensional (y_*, q_T) distribution for $\sqrt{s}$ = 7 TeV and $k_{T+}, k_{T-} >$ 3 GeV for MSTW08 PDF and KMR (left) and KS (right) UGDF.

Full rapidity range

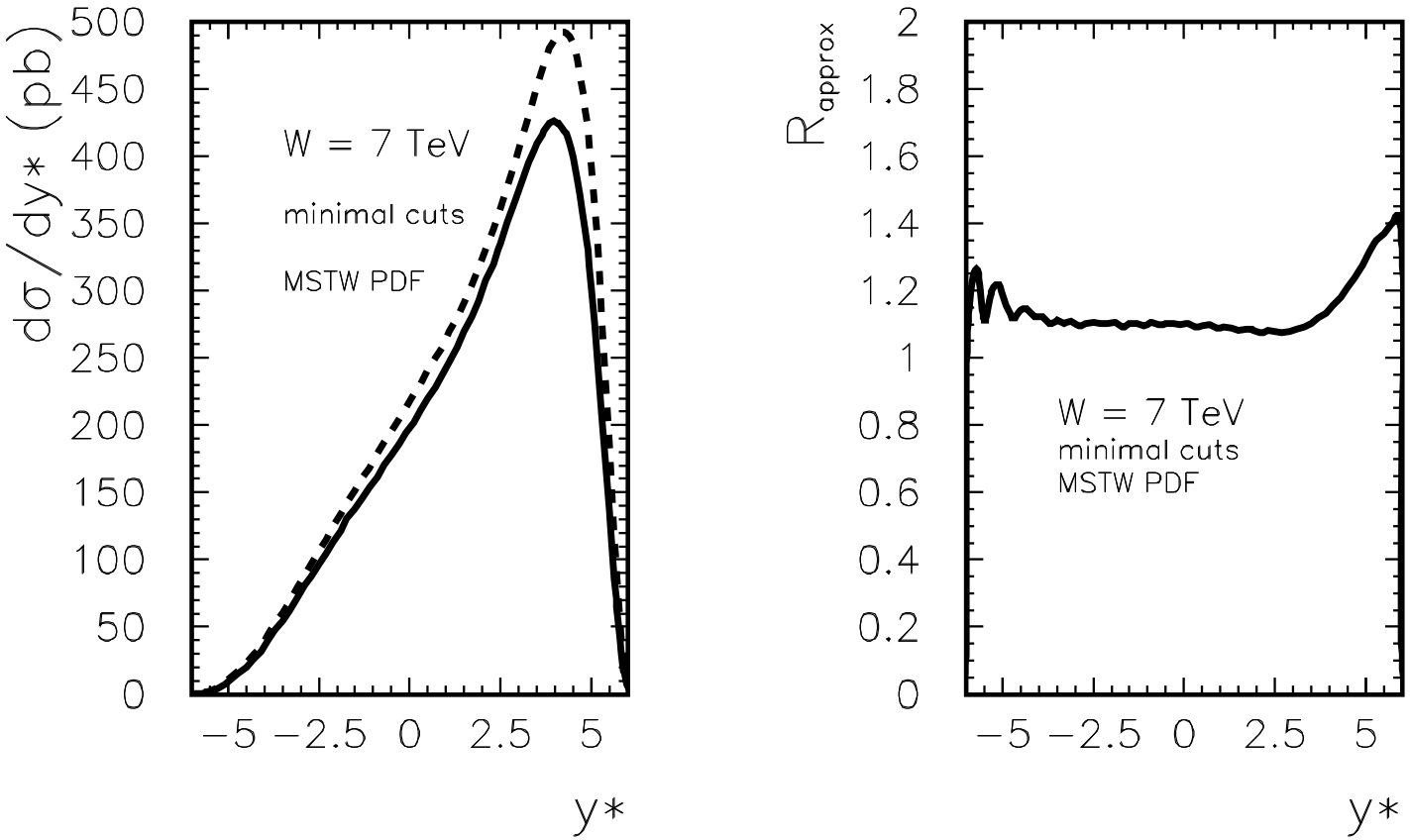

Figure: Distribution in y_* for exact (solid) and approximate (dashed) formula for calculating x_1 and x_2 for $\sqrt{s}$ = 7 TeV and $k_{T+}, k_{T-} > 3$ GeV for MSTW08 PDF and KMR UGDF. In the right panel we show the ratio of the two distributions.

Full rapidity range

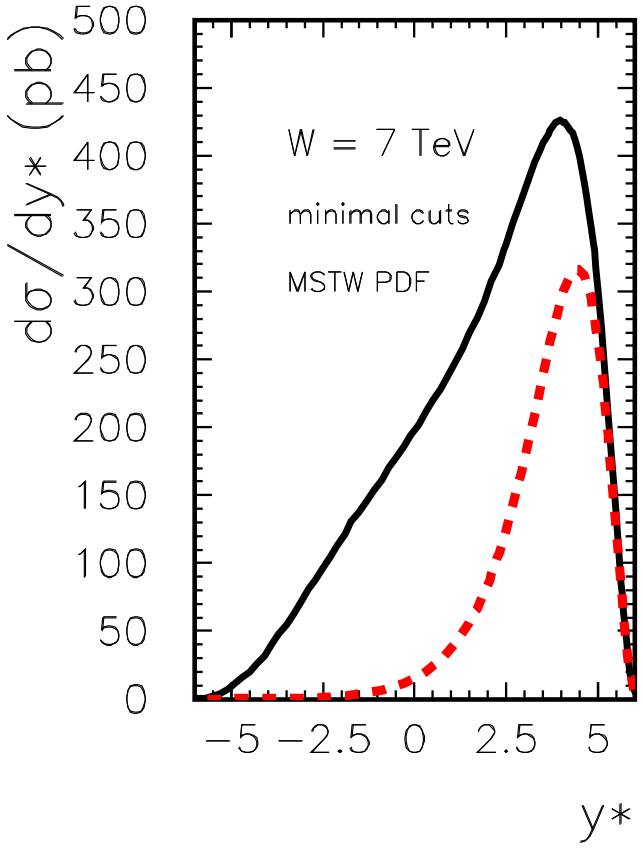

Figure: Distribution in rapidity of the dileptons for $\sqrt{s}$ = 7 TeV and $k_{T+}, k_{T-} >$ 3 GeV for MSTW08 valence quark distributions and KMR UGDF. The dashed line is the contribution from valence quarks only.

Forward region - LHCb

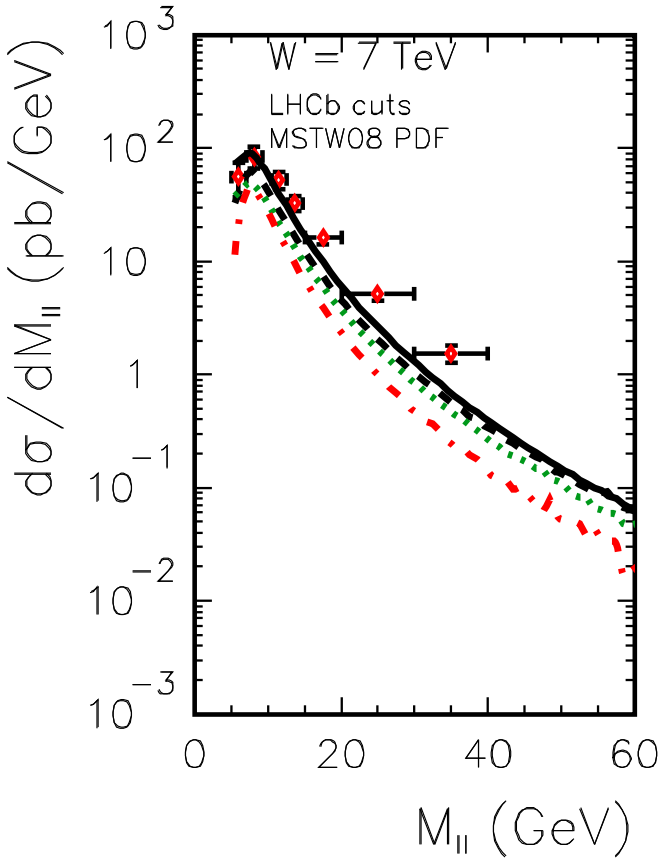

Figure: Invariant mass distribution (only the dominant component) for the LHCb cuts: $2 < y_+, y_- < 4.5$, $k_{T+}, k_{T-} > 3$ GeV for different UGDFs: KMR (solid), Kutak-Stasto (dashed), AAMS (dotted) and GBW (dash-dotted).

Forward region - LHCb

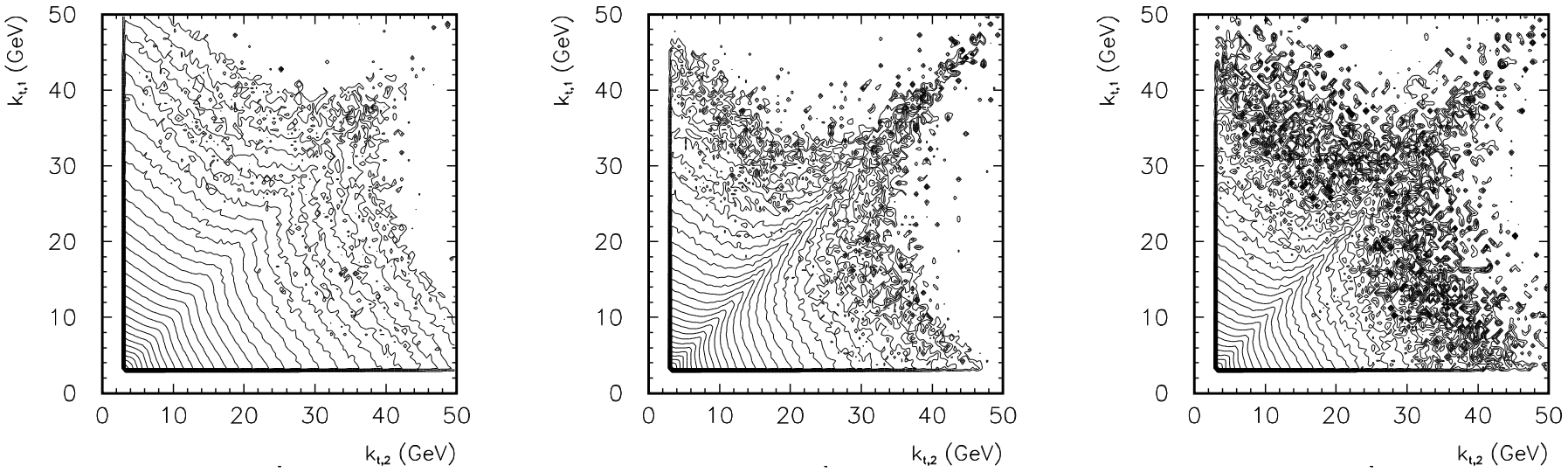

Figure: Two-dimensional (k_{T+}, k_{T-}) distribution for $\sqrt{s}$ = 7 TeV and $k_{T+}, k_{T-} >$ 3 GeV for MSTW08 PDF and KMR (left), KS (middle) and AAMS (right) UGDFs.

Forward region - LHCb

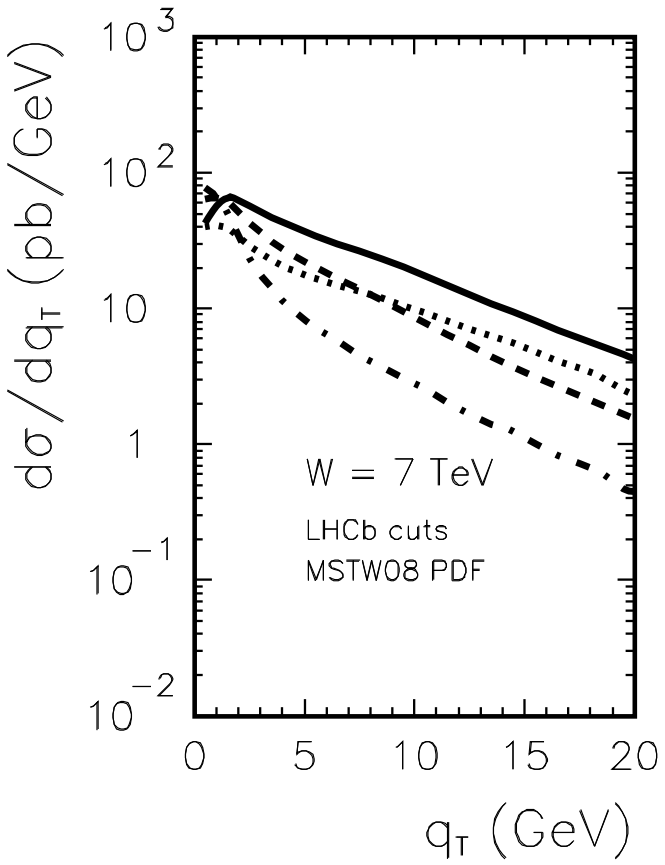

Figure: Dilepton transverse momentum distribution (only the dominant component) for the LHCb cuts: $2 < y_+, y_- < 4.5$, $k_{T+}, k_{T-} > 3$ GeV for different UGDFs: KMR (solid), Kutak-Stasto (dashed), AAMS (dotted) and GBW (dash-dotted).

Forward region - LHCb

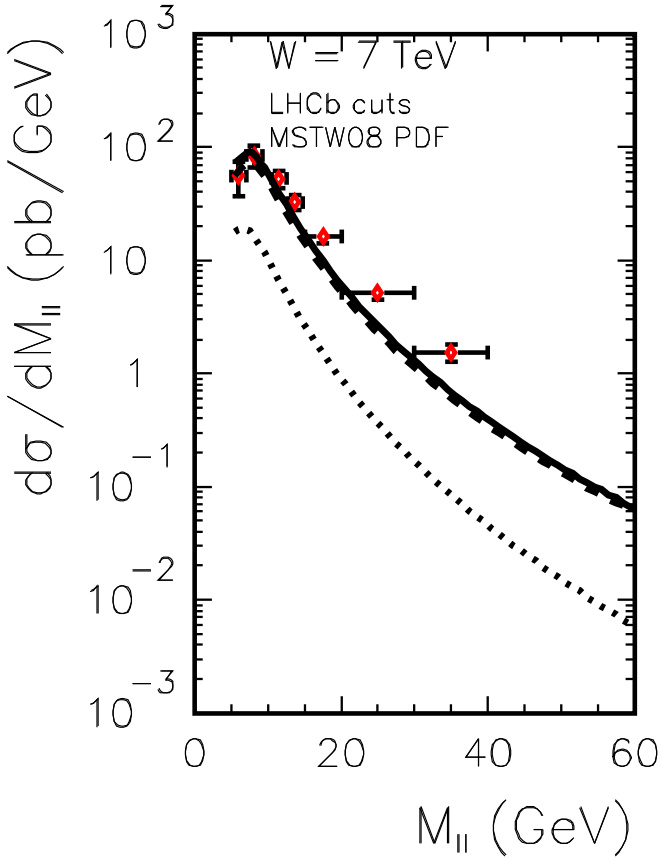

Figure: The T and L contributions to the dilepton invariant mass distribution for the LHCb kinematics: $2 < y_+, y_- < 4.5$, $k_{T+}, k_{T-} > 3$ GeV. KMR UGDF was used here.

Forward region - LHCb

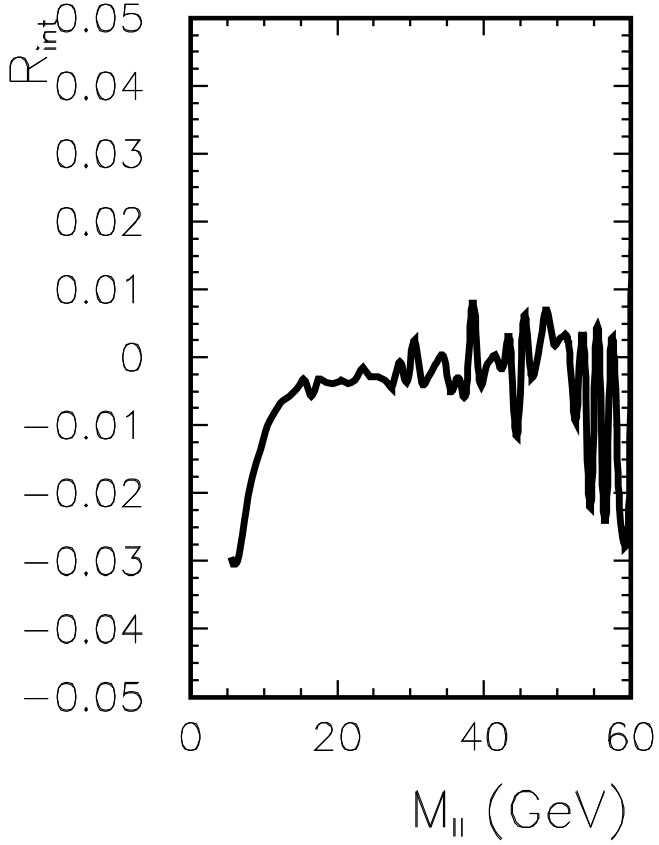

Figure: The R_{int} as a function of M_{ll} for the LHCb kinematics: $2 < y_+, y_- < 4.5$, $k_{T+}, k_{T-} > 3$ GeV. KMR UGDF was used here. The fluctuations are due to insufficient statistics of our Monte Carlo calculation.

$$R_{int} = \frac{d\sigma_{all} - d\sigma_{T+L}}{d\sigma_{all}} \,. \tag{11}$$

Forward region - LHCb

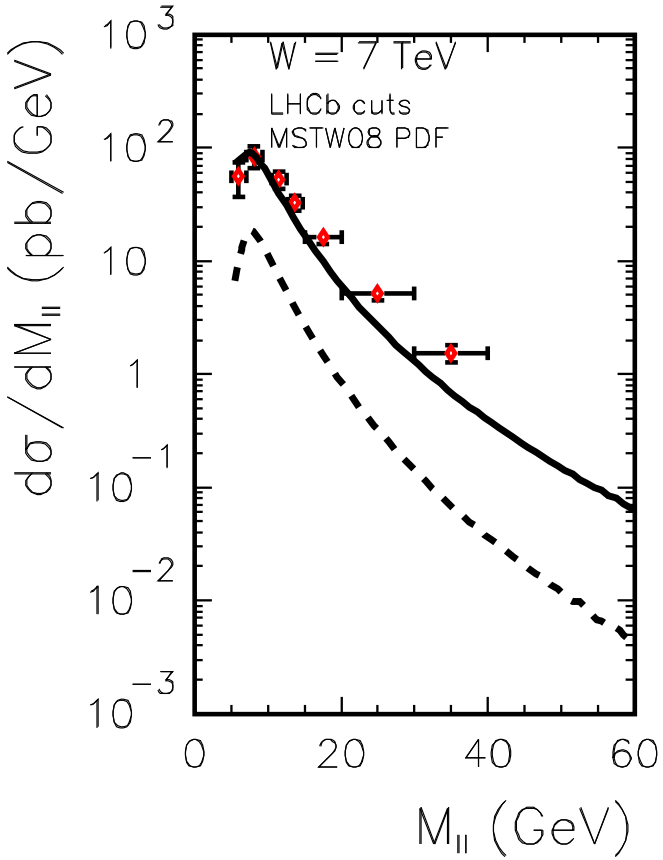

Figure: Contributions of the second-side component for the LHCb kinematics: $2 < y_+, y_- < 4.5$, $k_{T+}, k_{T-} > 3$ GeV. KMR UGDF was used here.

Midrapidity region - ATLAS

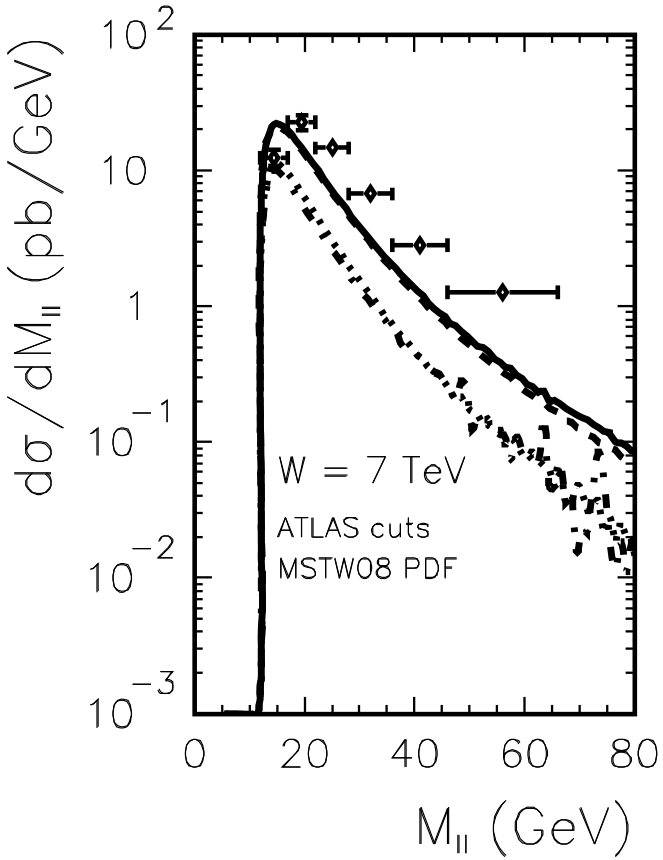

Figure: Invariant dilepton mass distribution for the ATLAS kinematics: -2.4 $< y_+, y_- <$ 2.4, $k_{T+}, k_{T-} >$ 6 GeV. Here both $gq/\bar{q}$ and $q/\bar{q}g$ contributions have been included.

Midrapidity region - ATLAS

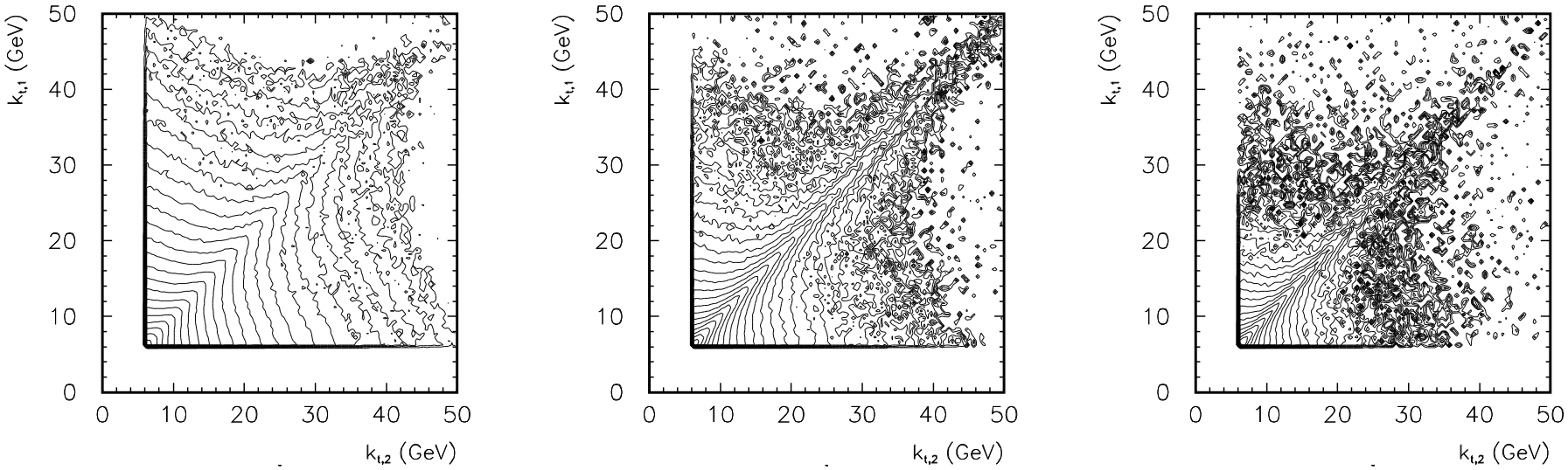

Figure: Lepton transverse momentum correlations for the ATLAS kinematics: -2.4 $< y_+, y_- <$ 2.4, $k_{T+}, k_{T-} >$ 6 GeV. The left panel is for the KMR UGDF, the middle panel for the KS UGDF and the right panel for the AAMS UGDF.

Midrapidity region - ATLAS

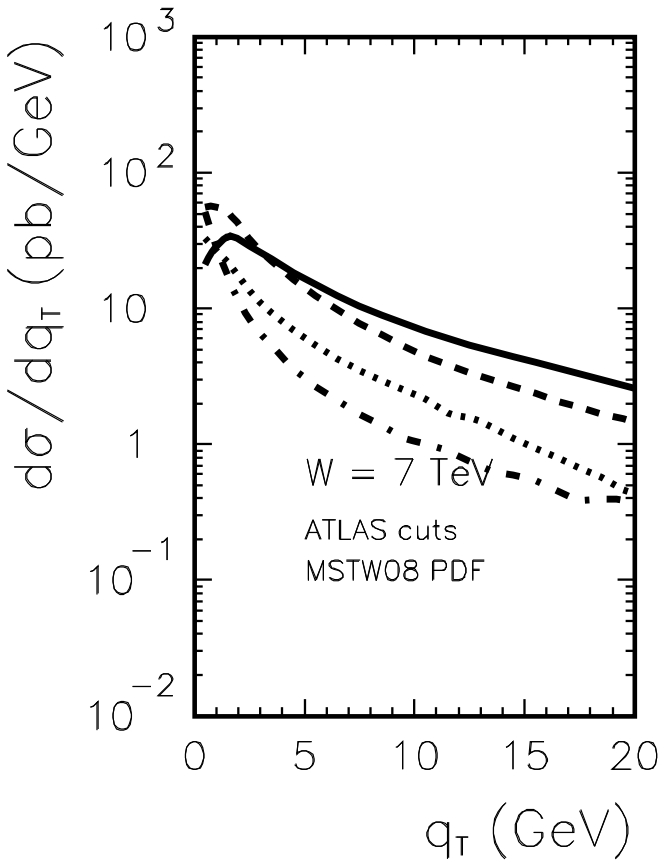

Figure: Transverse momentum distribution of dileptons for the ATLAS kinematics: -2.4 $< y_+, y_- <$ 2.4, $k_{T+}, k_{T-} >$ 6 GeV for MWST08 PDF and for different UGDFs: KMR (solid), KS (dashed), AAMS (dotted) and GBW (dash-dotted).

$pp \to ppJ/\psi$

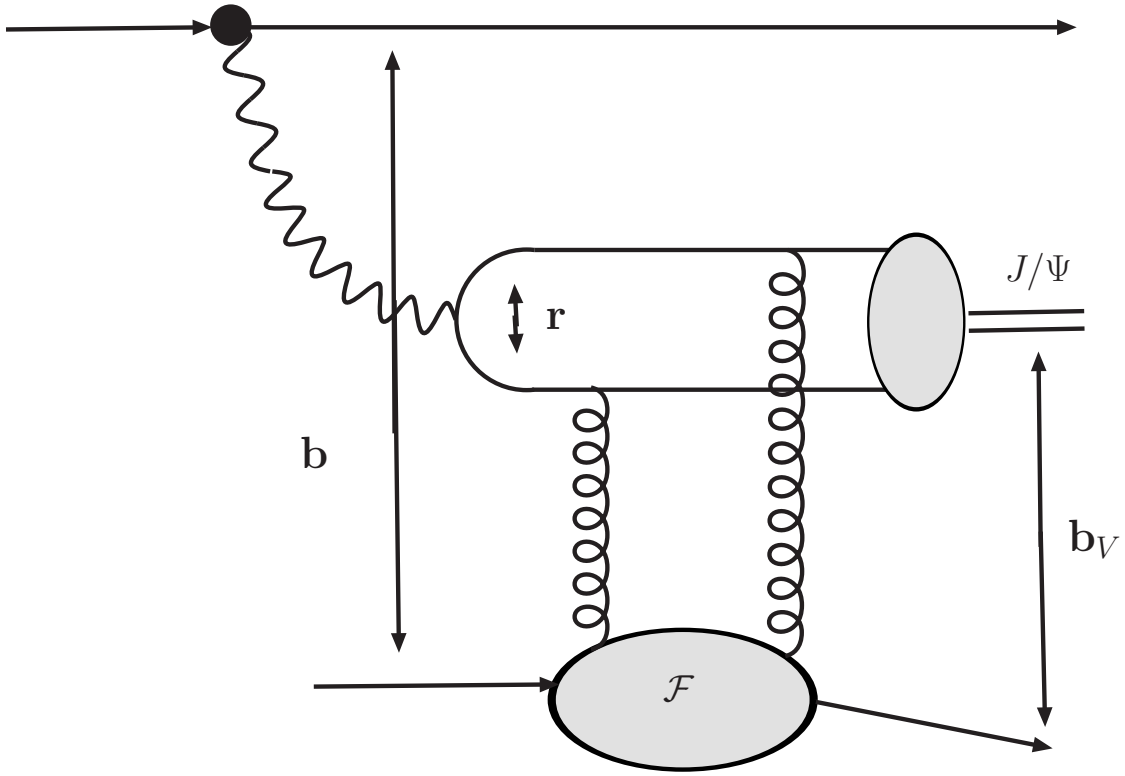

A. Cisek, W. Schäfer and A. Szczurek, JHEP **1504** (2015) 159.

$pp \to ppJ/\psi$

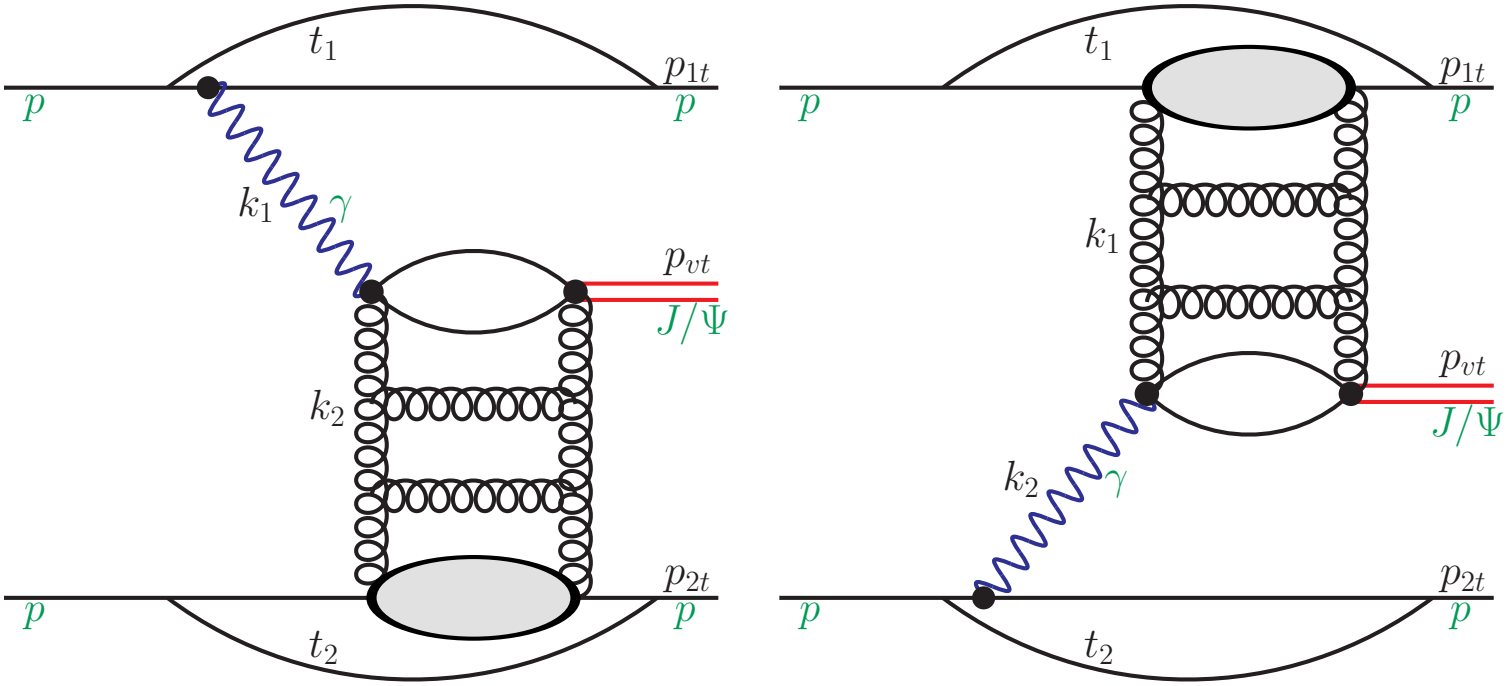

The interference term vanishes for rapidity distributions in Born approximation

see W. Schäfer and A. Szczurek, Phys. Rev. **D76** (2007) 094014.

$pp \to ppJ/\psi$

Imaginary part of the forward $\gamma p \to J/\psi p$ amplitude

$$\Im m\, \mathcal{M}_T(W, \Delta^2 = 0, Q^2 = 0) = W^2 \frac{c_v \sqrt{4\pi\alpha_{em}}}{4\pi^2}\, 2 \int_0^1 \frac{dz}{z(1-z)} \int_0^\infty \pi dk^2 \psi_V(z, k$$

$$\int_0^\infty \frac{\pi d\kappa^2}{\kappa^4} \alpha_S(q^2) \mathcal{F}(x_{\rm eff}, \kappa^2) \Big(A_0(z, k^2)\, W_0(k^2, \kappa^2) + A_1(z, k^2)\, W_1(k^2, \kappa^2)$$

dependence on the meson wave function and UGDF
No wave functions in collinear calculations (Jones, Martin, Ryskin)

The full amplitude, at finite momentum transfer parametrized:

$$\mathcal{M}(W, \Delta^2) = (i + \rho)\, \Im m \mathcal{M}(W, \Delta^2 = 0, Q^2 = 0)\, \exp(-B(W)\Delta^2/2)\,, (13$$

$pp \to ppJ/\psi$

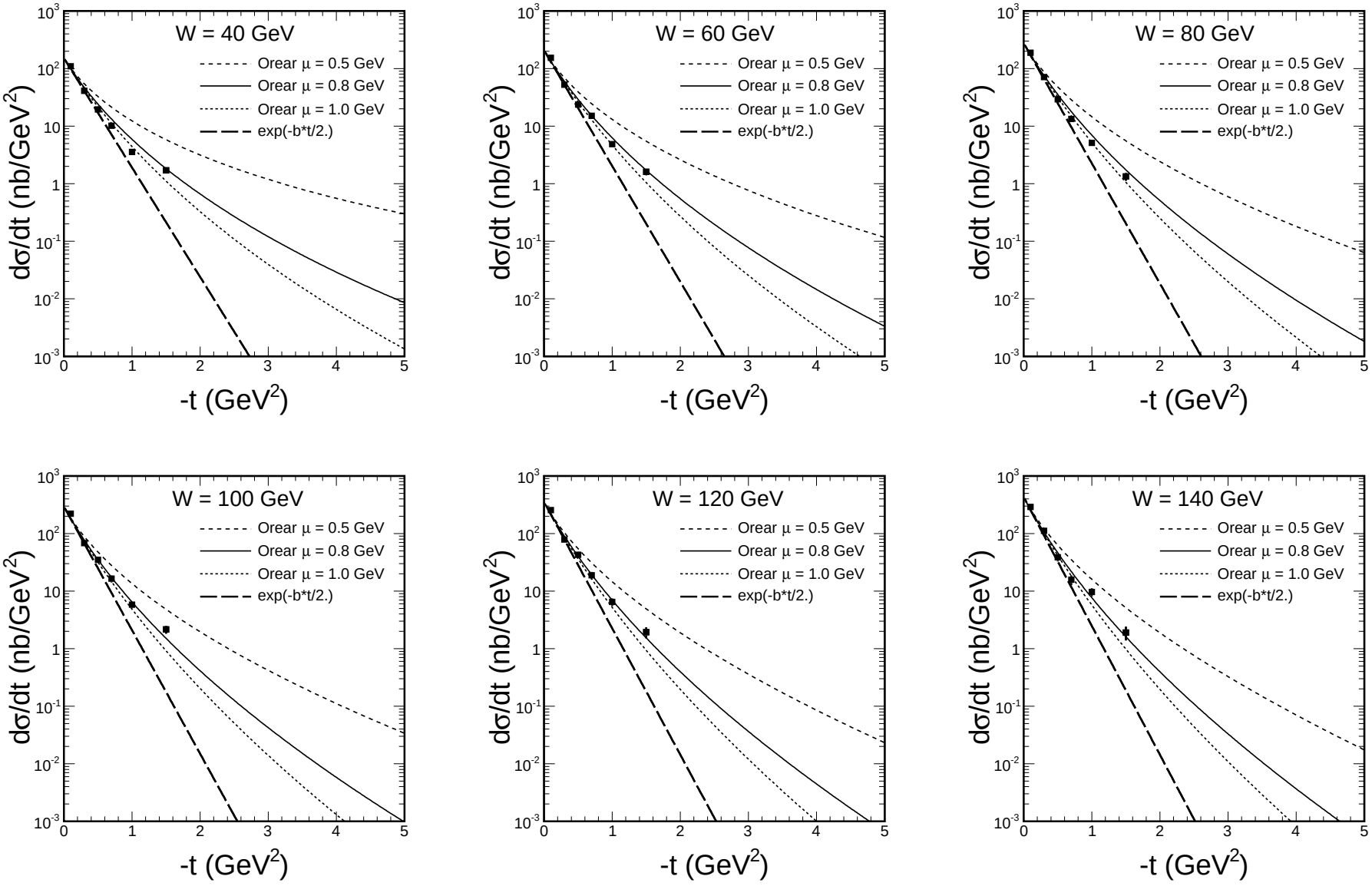

Deviations from exponential t dependence

$pp \to ppJ/\psi$

In the Born approximation:

$$\mathcal{M}^{\lambda_1\lambda_2\to\lambda_1'\lambda_2'\lambda_V}_{h_1h_2\to h_1h_2V}(s,s_1,s_2,t_1,t_2) = \mathcal{M}_{\gamma\mathbf{P}} + \mathcal{M}_{\mathbf{P}\gamma}$$

$$= \langle p_1',\lambda_1'|J_\mu|p_1,\lambda_1\rangle \epsilon^*_\mu(q_1,\lambda_V)\frac{\sqrt{4\pi\alpha_{em}}}{t_1}\mathcal{M}^{\lambda_{\gamma^*}\lambda_2\to\lambda_V\lambda_2}_{\gamma^*h_2\to Vh_2}(s_2,t_2,Q_1^2)$$

$$+\langle p_2',\lambda_2'|J_\mu|p_2,\lambda_2\rangle \epsilon^*_\mu(q_2,\lambda_V)\frac{\sqrt{4\pi\alpha_{em}}}{t_2}\mathcal{M}^{\lambda_{\gamma^*}\lambda_1\to\lambda_V\lambda_1}_{\gamma^*h_1\to Vh_1}(s_1,t_1,Q_2^2)\,. \quad (14)$$

$pp \to ppJ/\psi$

Then, the amplitude of Eq. (14) for the emission of a photon of transverse polarization λ_V, and transverse momentum $\boldsymbol{q}_1 = -\boldsymbol{p}_1$ can be written as:

$$\langle p_1', \lambda_1' | J_\mu | p_1, \lambda_1 \rangle \epsilon_\mu^*(q_1, \lambda_V)$$
$$= \frac{(\boldsymbol{e}^{*(\lambda_V)} \boldsymbol{q}_1)}{\sqrt{1 - z_1}} \frac{2}{z_1} \chi_{\lambda'}^\dagger \left\{ F_1(Q_1^2) - \frac{i \kappa_p F_2(Q_1^2)}{2 m_p} (\boldsymbol{\sigma}_1 \cdot [\boldsymbol{q}_1, \boldsymbol{n}]) \right\} \chi_\lambda \,. \quad (15)$$

F_1 - Dirac em ff
F_2 - Pauli em ff (new)

$pp \to ppJ/\psi$

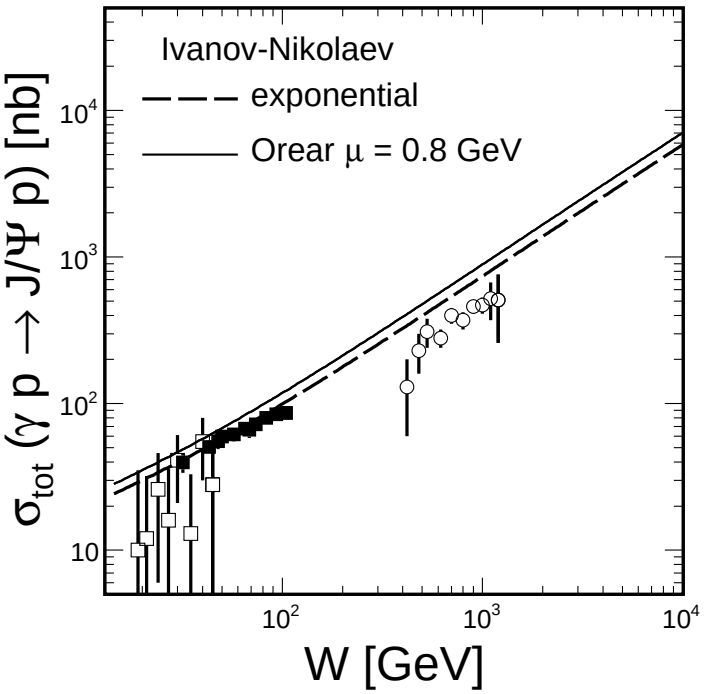

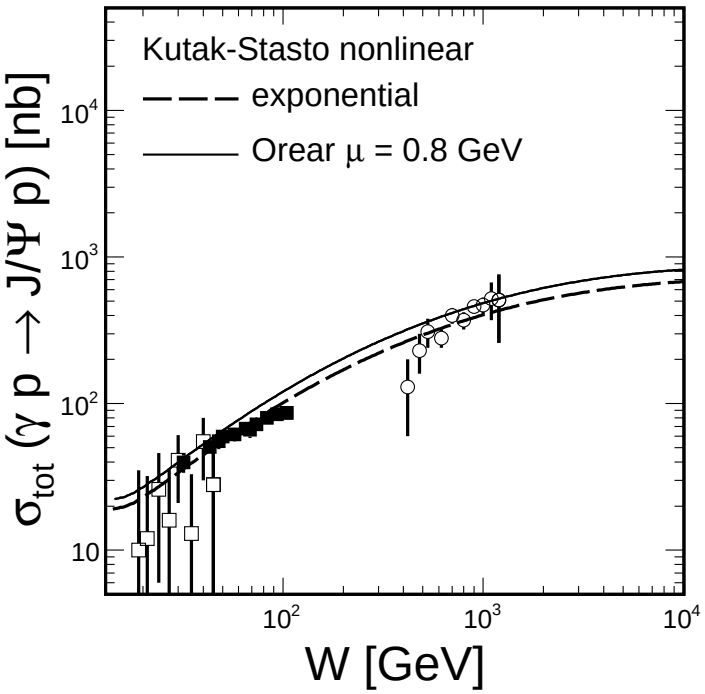

HERA data at W $\sim$ 100-200 GeV
LHCb quasi-data at W $\sim$ 1 TeV

$pp \to ppJ/\psi$

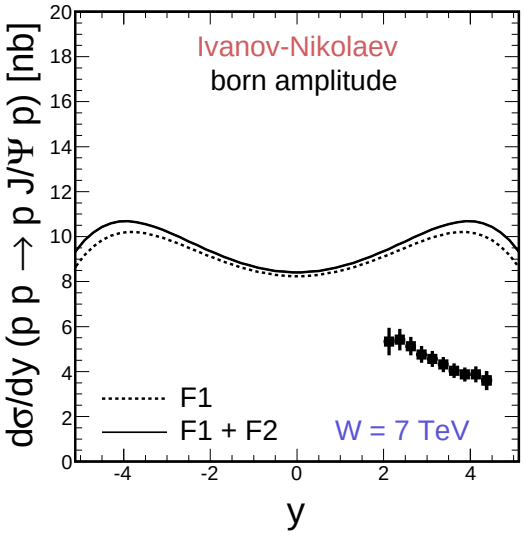
Ivanov-Nikolaev
born amplitude
F1
F1 + F2
W = 7 TeV
dσ/dy (p p → p J/Ψ p) [nb]
y

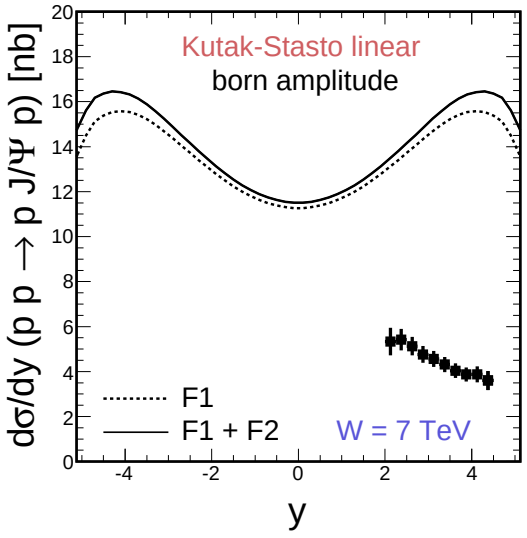
Kutak-Stasto linear
born amplitude
F1
F1 + F2
W = 7 TeV
dσ/dy (p p → p J/Ψ p) [nb]
y

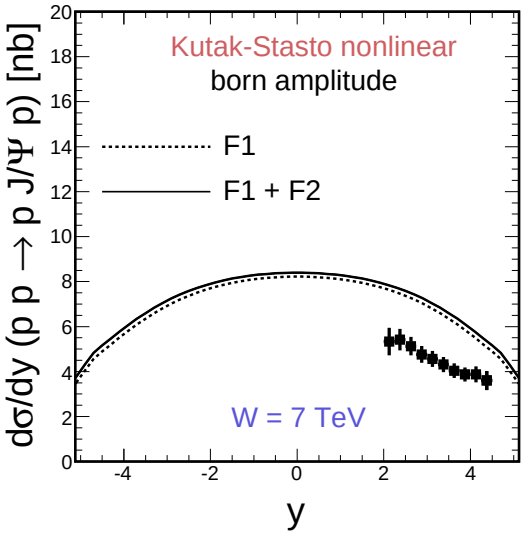
Kutak-Stasto nonlinear
born amplitude
F1
F1 + F2
W = 7 TeV
dσ/dy (p p → p J/Ψ p) [nb]
y

$pp \to ppJ/\psi$

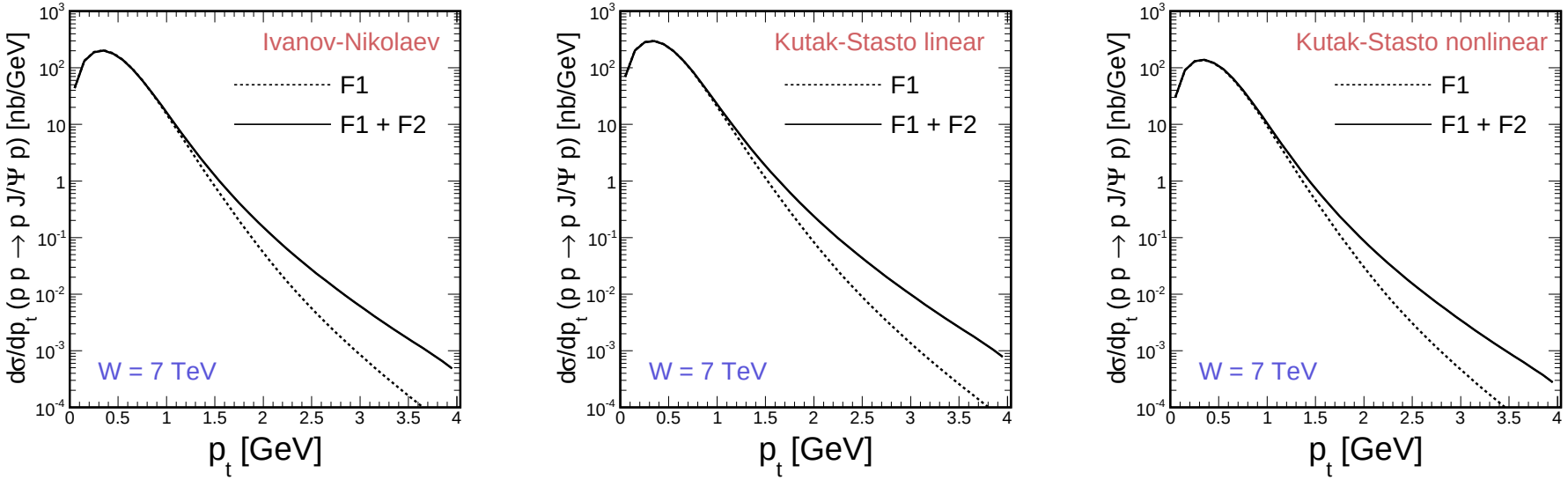
Ivanov-Nikolaev
F1
F1 + F2
W = 7 TeV
Kutak-Stasto linear
F1
F1 + F2
W = 7 TeV
Kutak-Stasto nonlinear
F1
F1 + F2
W = 7 TeV
dσ/dp_t (p p → p J/Ψ p) [nb/GeV]
p_t [GeV]

$pp \to ppJ/\psi$

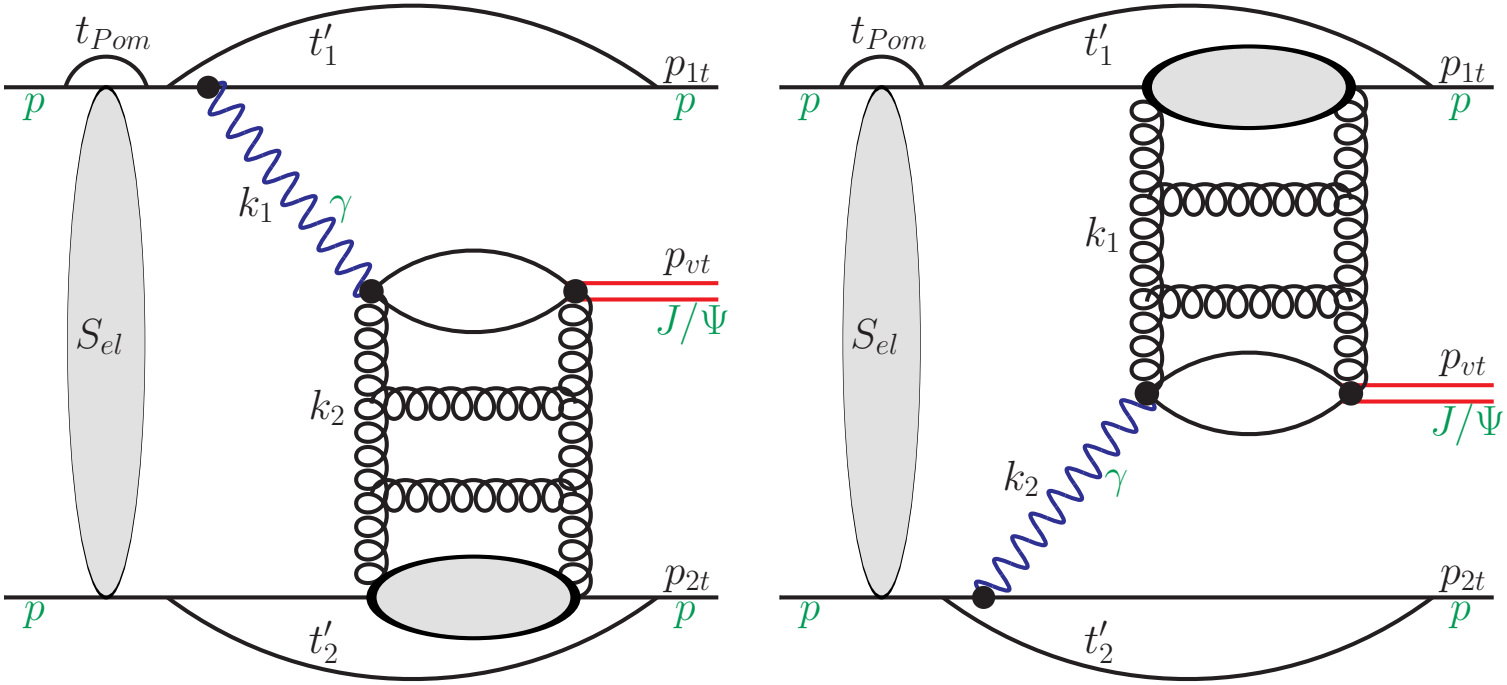

Survival factor depends on the phase space point !

$pp \to ppJ/\psi$

with absorption

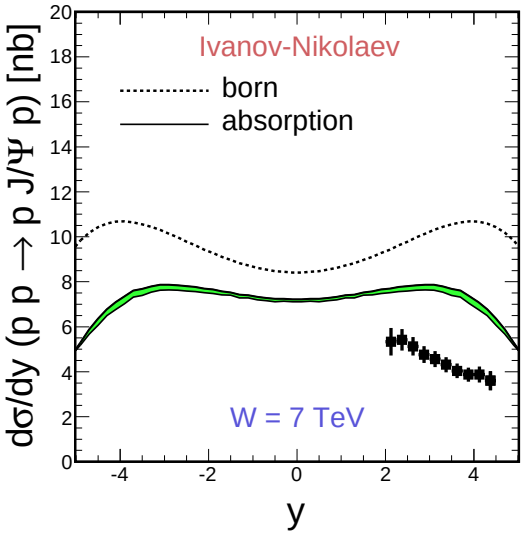

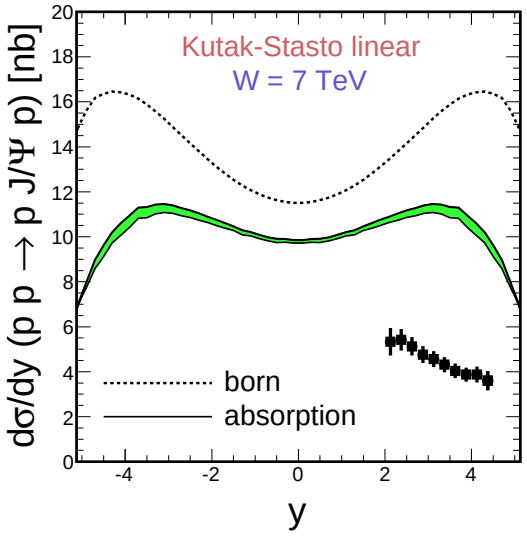

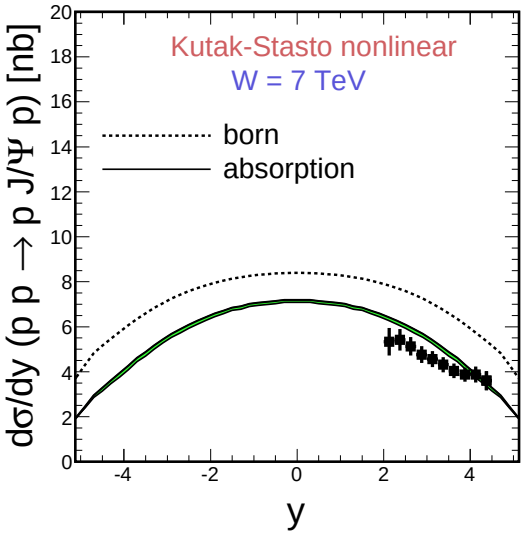

similar for ψ'

$pp \to ppJ/\psi$

with absorption

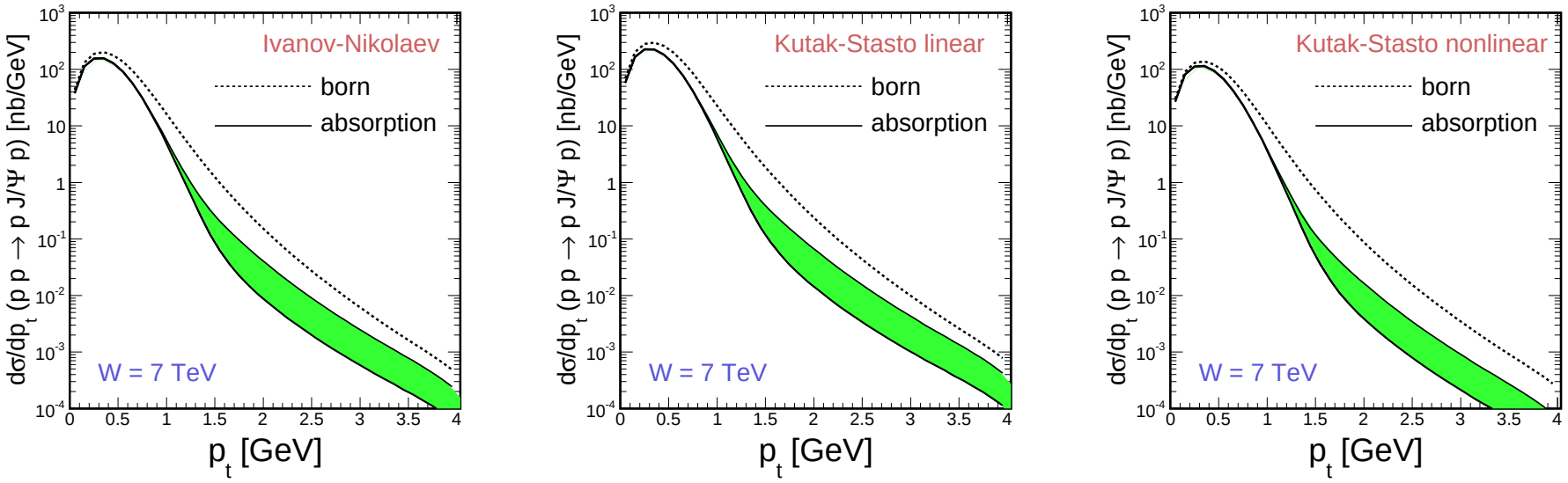

similar for ψ'

ψ' to J/ψ ratio

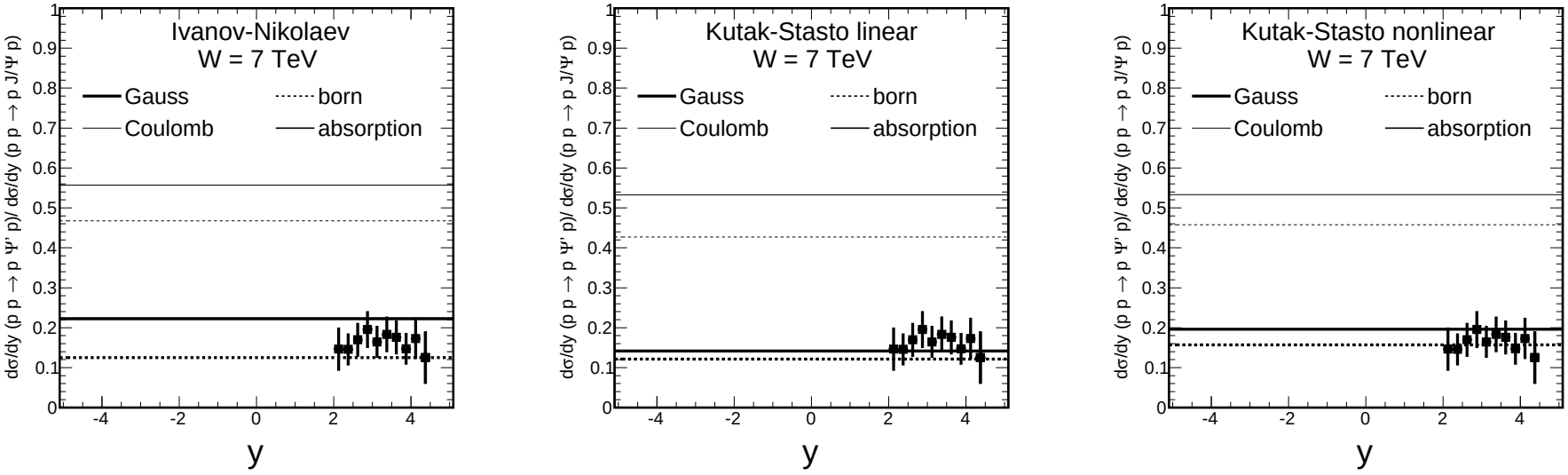

Gauss WF much better than Coulomb WF

Semiexclusive production, electromagnetic excitation

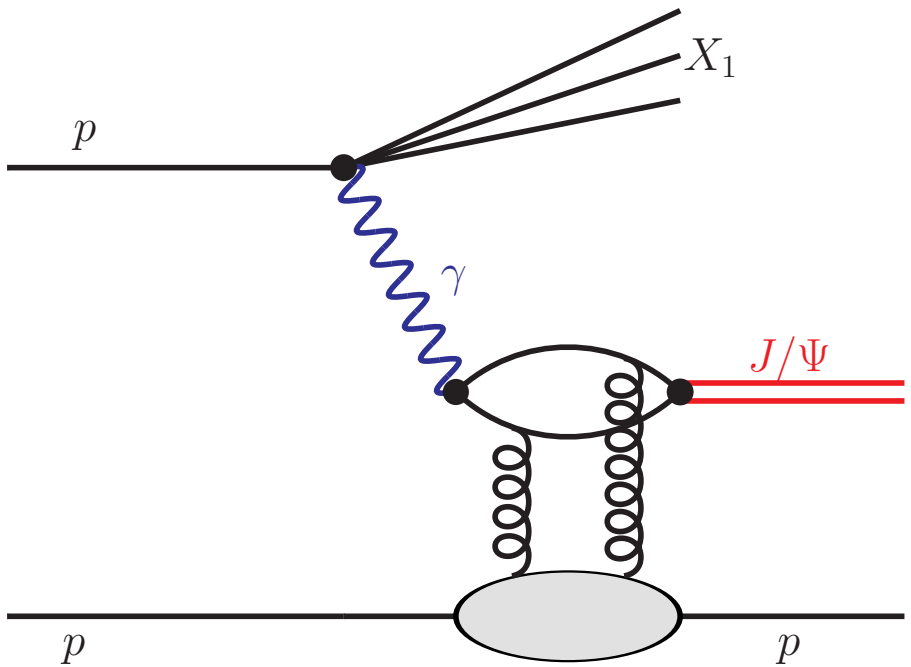

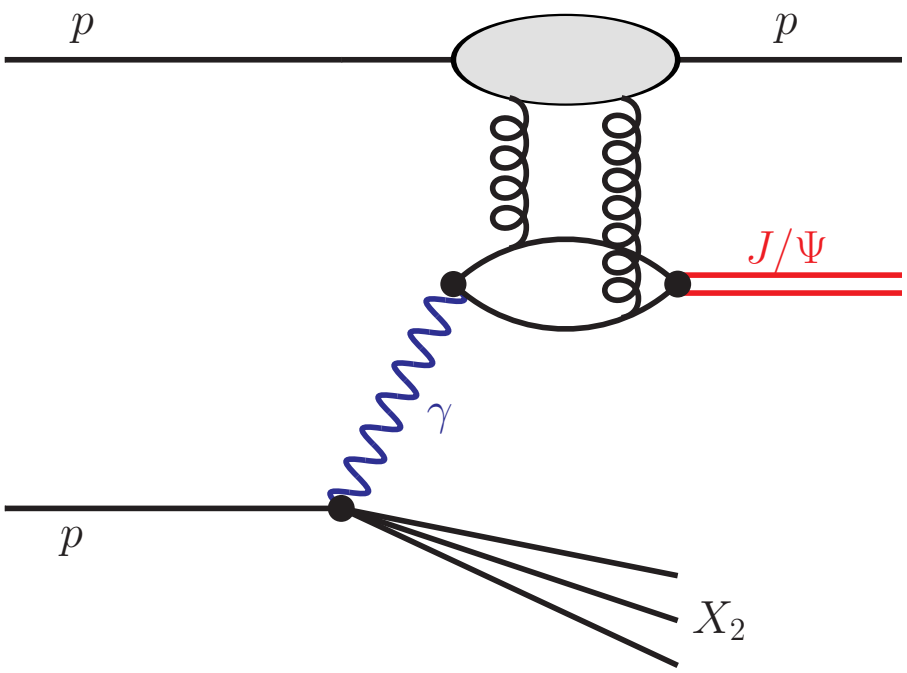

One-side excitation only

A. Cisek, W. Schäfer and A. S., arXiv:1611.08210

Electromagnetic excitation

The cross section for such processes can be written as:

$$\frac{d\sigma(pp \to XVp; s)}{dyd^2\boldsymbol{p}dM_X^2} = \int \frac{d^2\boldsymbol{q}}{\pi \boldsymbol{q}^2} \mathcal{F}^{(\mathrm{inel})}_{\gamma/p}(z_+, \boldsymbol{q}^2, M_X^2) \frac{1}{\pi} \frac{d\sigma^{\gamma^* p \to Vp}}{dt}(z_+ s, t = -(\boldsymbol{q} - \boldsymbol{p})^2$$

where $z_\pm = e^{\pm y}\sqrt{(\boldsymbol{p}^2 + m_V^2)/s}$.

$$\mathcal{F}^{(\mathrm{inel})}_{\gamma/p}(z, \boldsymbol{q}^2, M_X^2) = \frac{\alpha_{\mathrm{em}}}{\pi}(1-z)\theta(M_X^2 - M_{\mathrm{thr}}^2)\frac{F_2(x_{Bj}, Q^2)}{M_X^2 + Q^2 - m_p^2}\left[\frac{\boldsymbol{q}^2}{\boldsymbol{q}^2 + z(M_X^2 - m_p^2)}\right.$$

where

$$Q^2 = \frac{1}{1-z}\left[\boldsymbol{q}^2 + z(M_X^2 - m_p^2) + z^2 m_p^2\right], x_{Bj} = \frac{Q^2}{Q^2 + M_X^2 - m_p^2}. \quad (18)$$

Semiexclusive production, resonance diffractive excitation

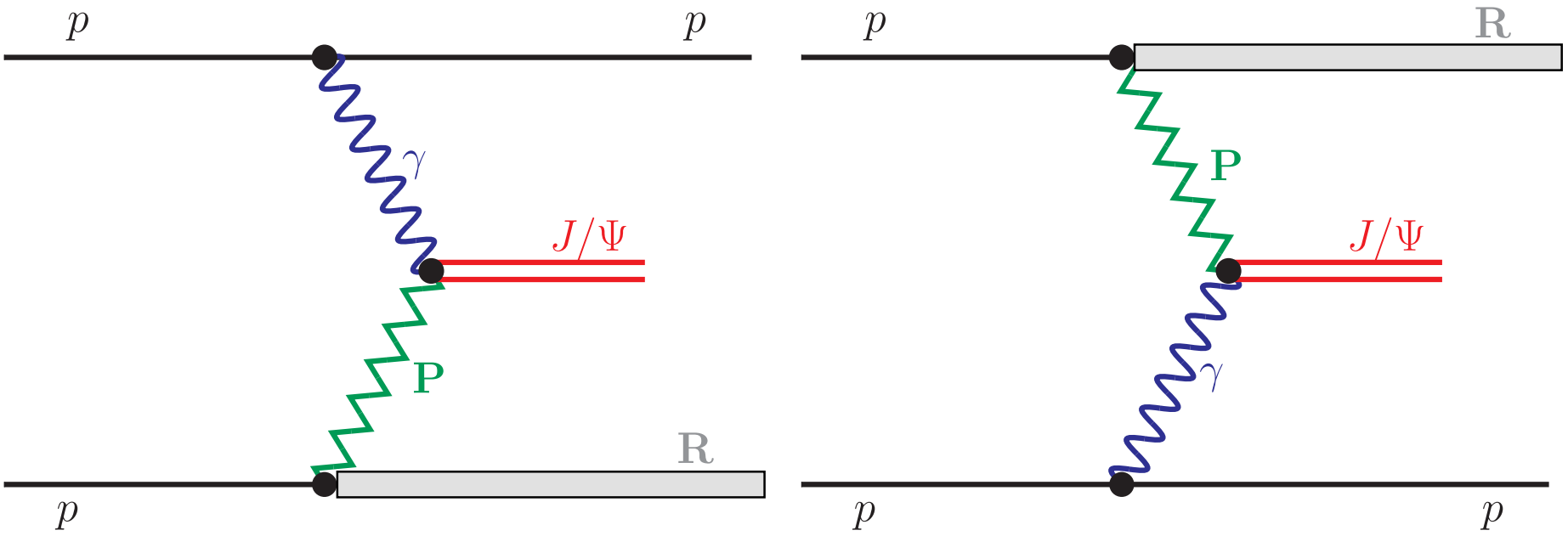

One-side excitation only

Diffractive resonance contribution

We consider Jenkovszky et al. dual Regge model.

The contribution of three positive-parity baryon resonances on the nucleon trajectory are taken into account:

1. N(1680), $J = \frac{5}{2}$
2. N(2220), $J = \frac{9}{2}$
3. N(2700), $J = \frac{13}{2}$

Their contribution is accounted for by

$$\Im m A(M_X^2, t) = \sum_{n=1,3} [f(t)]^{2(n+1)} \cdot \frac{\Im m\, \alpha(M_X^2)}{(J_n - \Re e\, \alpha(M_X^2))^2 + (\Im m\, \alpha(M_X^2))^2}. \quad (19)$$

Here J_n is the spin of the nth resonance, and the explicit form of the complex Regge trajectory $\alpha(M_X^2)$ as well as the form factor $f(t)$ are from Jenkovszky et al.

We can now compute the contribution from diffractive excitation of small masses from:

$$\frac{d\sigma(pp \to XVp; s)}{dy d^2\boldsymbol{p} dM_X^2} = \int \frac{d^2\boldsymbol{q}}{\pi \boldsymbol{q}^2} \mathcal{F}^{(\mathrm{el})}_{\gamma/p}(z_+, \boldsymbol{q}^2) \frac{1}{\pi} \frac{d\sigma(\gamma p \to VX)}{dt dM_X^2}(z_+ s) + (z_+ \leftrightarrow z_-), ($$

Semiexclusive production, partonic diffractive excitation

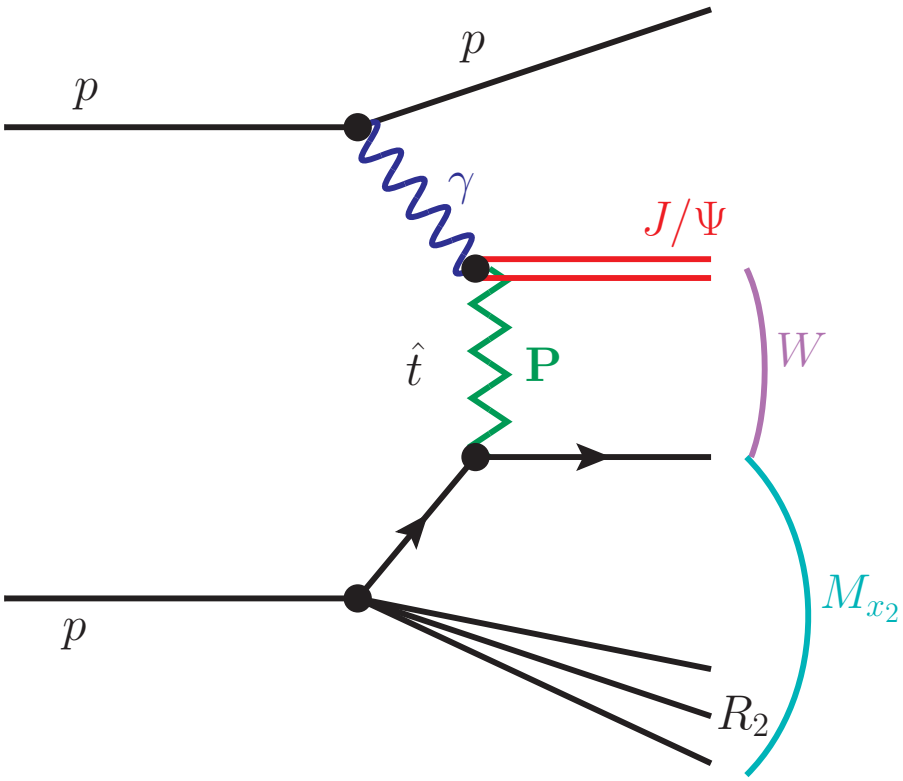

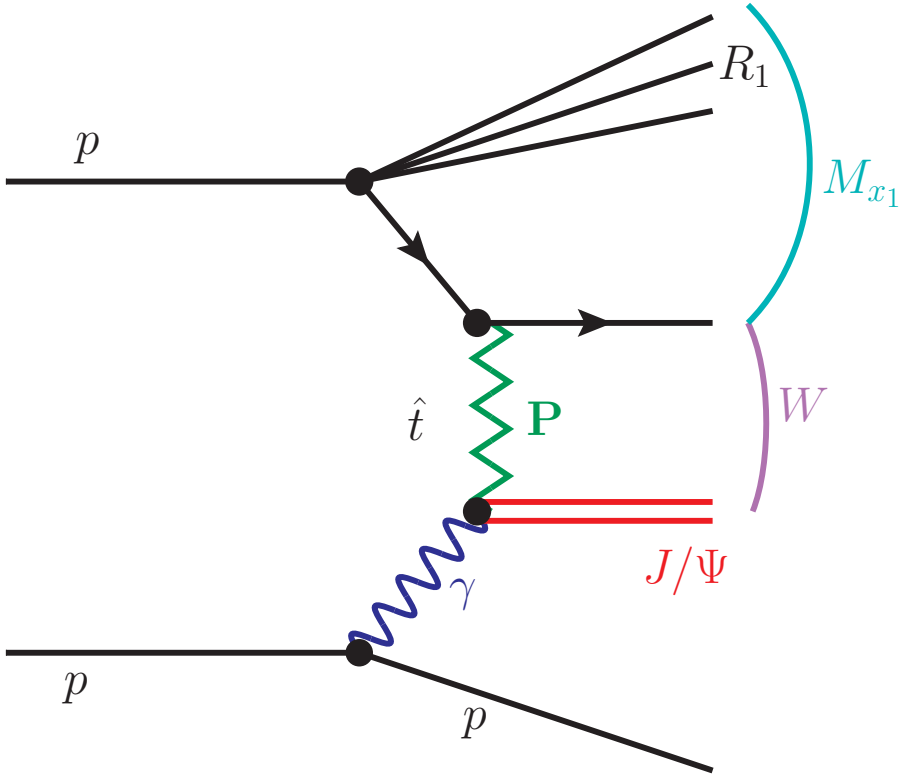

One-side excitation only

P means here two-gluon exchange

Diffractive partonic excitation

We neglect transverse momenta of the photon and intial quark/antiquark. In this approximation:

$$\frac{d\sigma^{diff,partonic}_{pp\to Vj}}{dy_V dy_j d^2p_t} = \frac{1}{16\pi^2\hat{s}^2} x_1 q_{eff}(x_1,\mu_F^2) x_2 \gamma_{el}(x_2) \overline{|\mathcal{M}_{q\gamma\to Vq}|^2} + \frac{1}{16\pi^2\hat{s}^2} x_1 \gamma_{el}(x_1) x_2 q_{eff}(x_2,\mu_F^2) \overline{|\mathcal{M}_{q\gamma\to Vq}|^2} \,. \quad (21)$$

The effective "quark" distribution reads as

$$q_{eff}(x,\mu_F^2) = \frac{81}{16} g(x,\mu_F^2) + \Sigma_f \left[q_f(x,\mu_F^2) + \bar{q}_f(x,\mu_F^2) \right] \,. \quad (22)$$

We take $\mu_F^2 = m_V^2 + |t|$ for the factorization scale. The matrix element for the partonic subprocess is related to the corresponding t-dependence as

$$\frac{d\sigma_{\gamma q\to Vq}}{dt} = \frac{1}{16\pi\hat{s}^2} \overline{|\mathcal{M}_{\gamma q\to Vq}|^2} \,. \quad (23)$$

In the following we shall use a simple formula for two-gluon exchange (Ivanov et al.) where

EM vs diffractive excitation

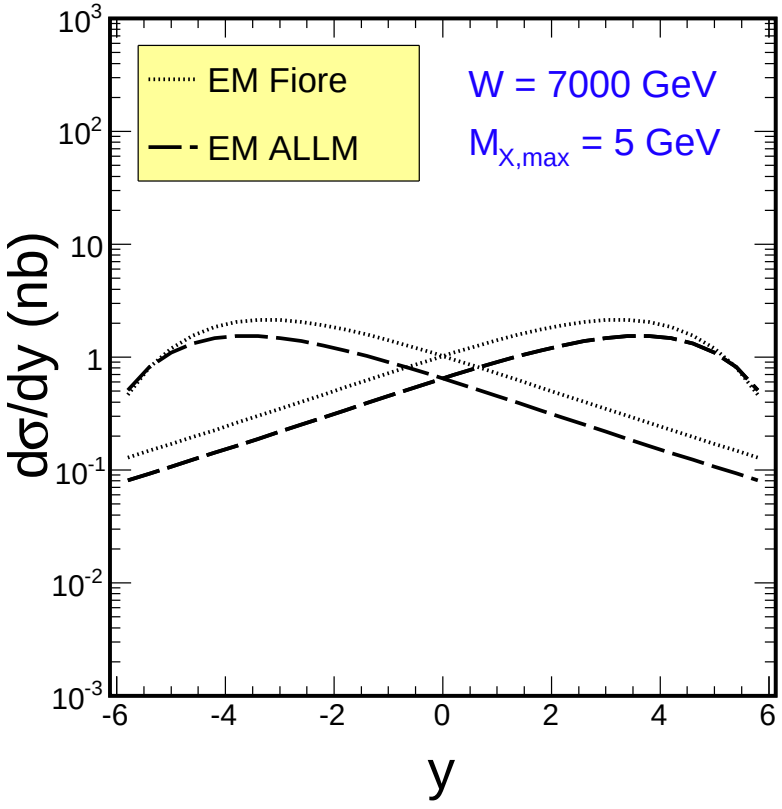

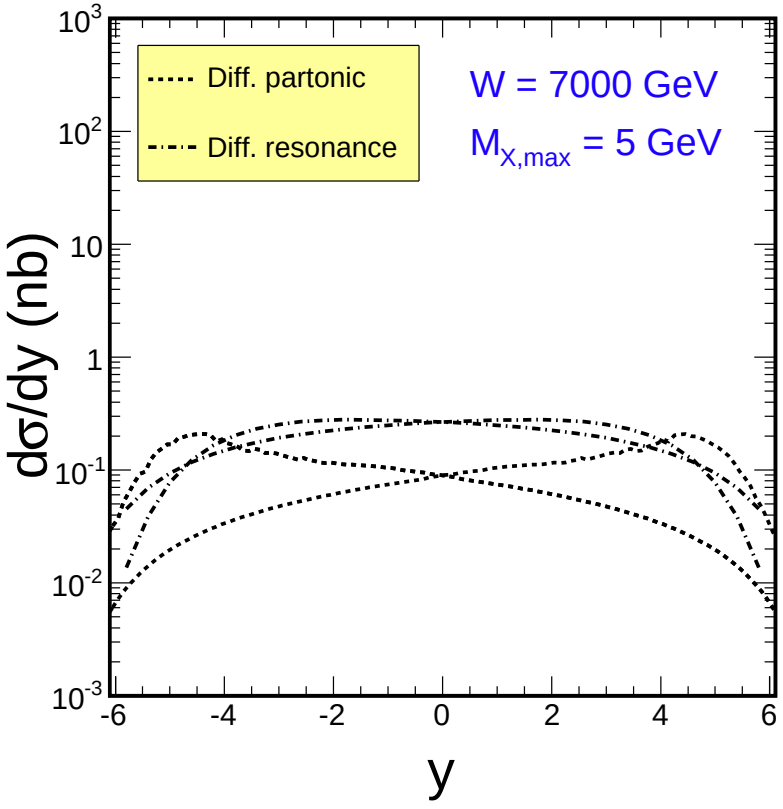

EM excitation contribution bigger than diffractive excitation contribution

Missing mass distribution

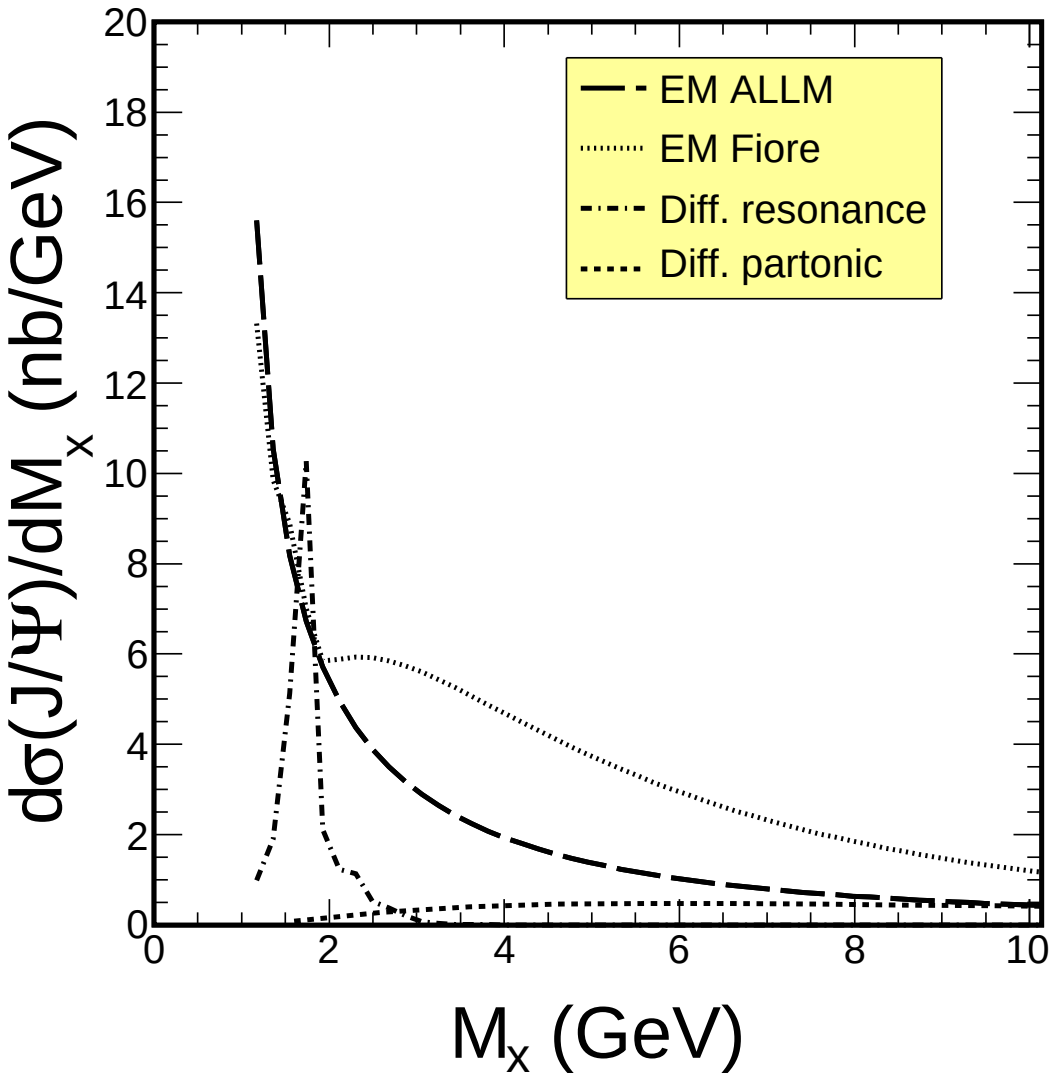

full phase space

Transverse momentum distribution for full phase space

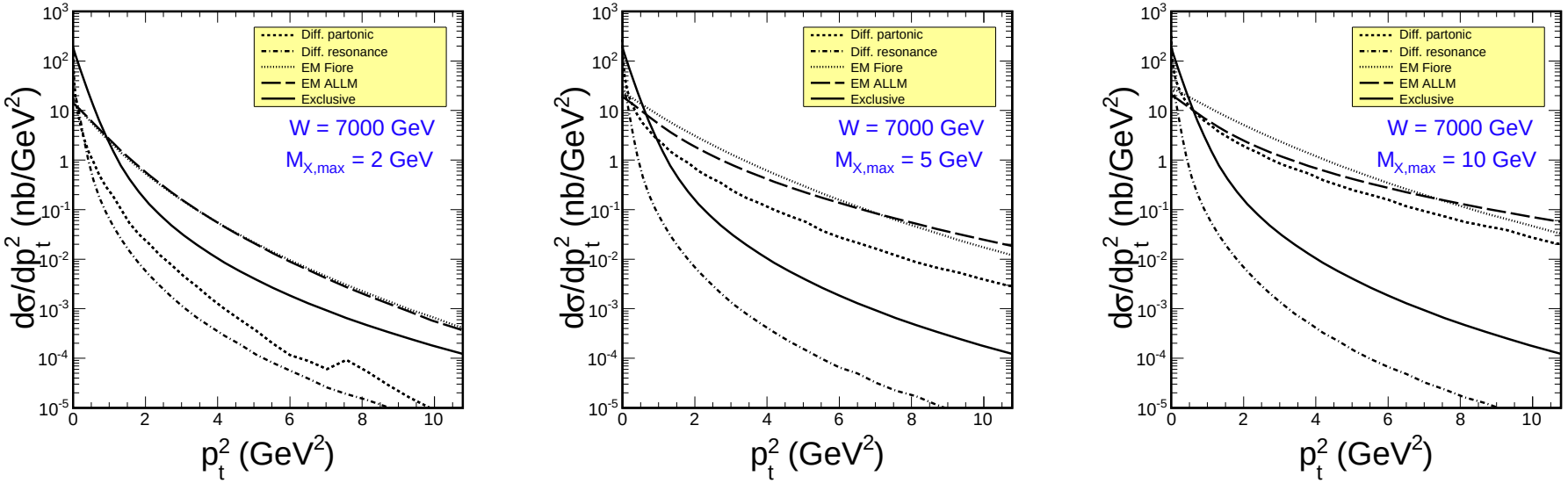

full phase space

Transverse momentum distribution for LHCb

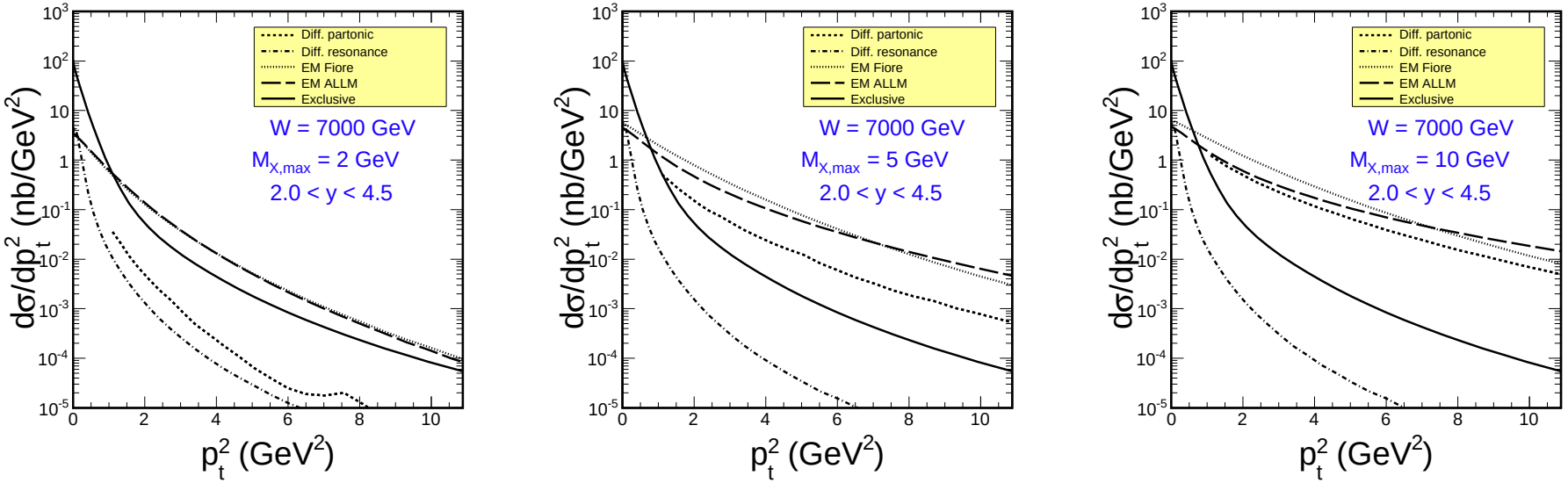

LHCb rapidity acceptance

Semi-exclusive to exclusive ratio

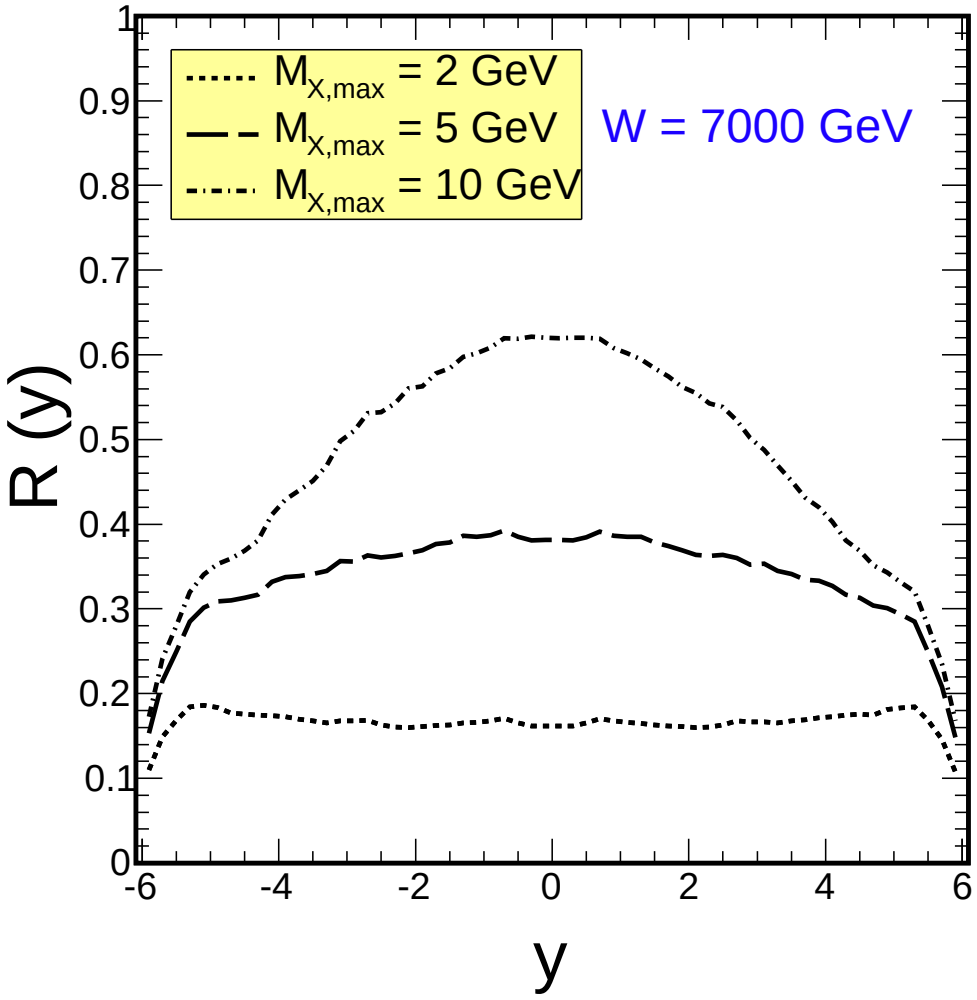

All dissociation processes

The ratio strongly depends on the range of missing masses

Inclusive J/ψ production

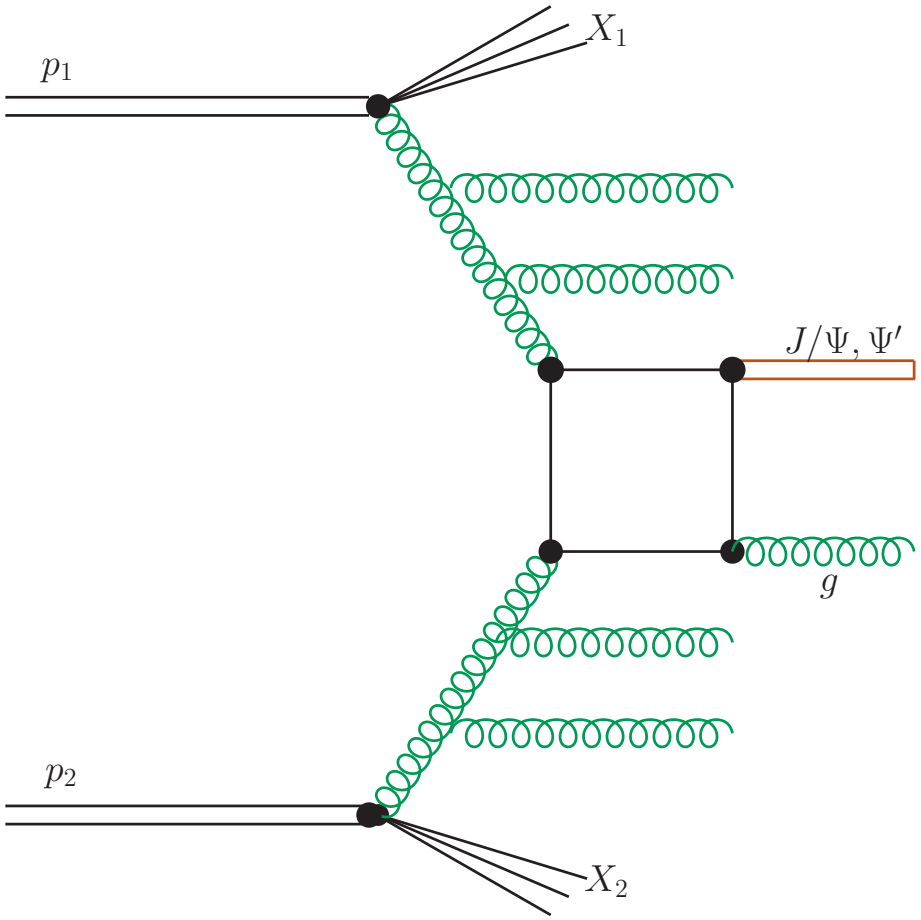

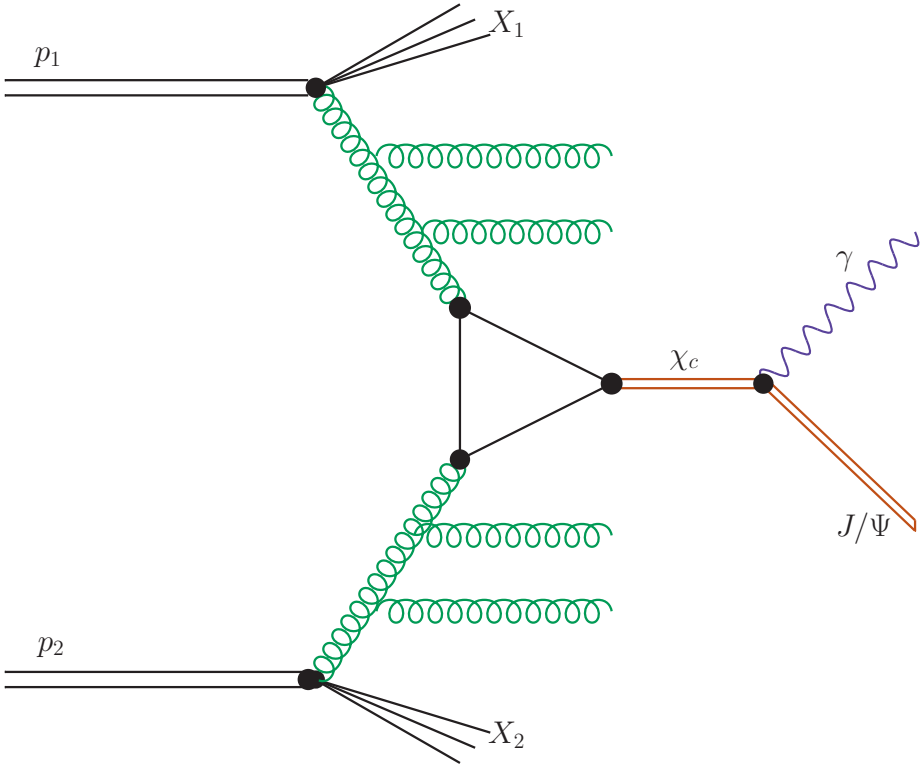

Inclusive J/ψ production

$$\frac{d\sigma(pp \to J/\psi g X)}{dy_{J/\psi} dy_g d^2p_{J/\psi,t} d^2p_{g,t}} = \frac{1}{16\pi^2 \hat{s}^2} \int \frac{d^2q_{1t}}{\pi} \frac{d^2q_{2t}}{\pi} \overline{|\mathcal{M}^{off-shell}_{g^*g^* \to J/\psi g}|^2}$$
$$\times \ \delta^2\left(\vec{q}_{1t} + \vec{q}_{2t} - \vec{p}_{H,t} - \vec{p}_{g,t}\right) \mathcal{F}_g(x_1, q_{1t}^2, \mu_F^2) \mathcal{F}_g(x_2, q_{2t}^2, \mu_F^2) \ . \quad (25)$$

The corresponding matrix element squared for the $gg \to J/\psi g$ is

$$|\mathcal{M}_{gg \to J/\psi g}|^2 \propto \alpha_s^3 |R(0)|^2 \ . \quad (26)$$

We use Baranov matrix elements

Inclusive χ_c production

In the k_t-factorization approach the leading-order cross section for the χ_c meson production can be written as:

$$\sigma_{pp\to\chi_c} = \int dy d^2p_t d^2q_t \frac{1}{sx_1x_2}\frac{1}{m^2_{t,\chi_c}}\overline{|\mathcal{M}_{g^*g^*\to\chi_c}|^2} \mathcal{F}_g(x_1,q^2_{1t},\mu^2_F)\mathcal{F}_g(x_2,q^2_{2t},\mu^2_F)/4 \,, \tag{27}$$

which can also be used to calculate rapidity and transverse momentum distributions of the χ_c mesons.
The matrix element squared for the $gg \to \chi_c$ subprocess is

$$|\mathcal{M}_{gg\to\chi_c}|^2 \propto \alpha_s^2|R'(0)|^2 \,. \tag{28}$$

We used the matrix element taken from the Kniehl, Vasin and Saleev paper.

χ_c contribution to inclusive J/ψ

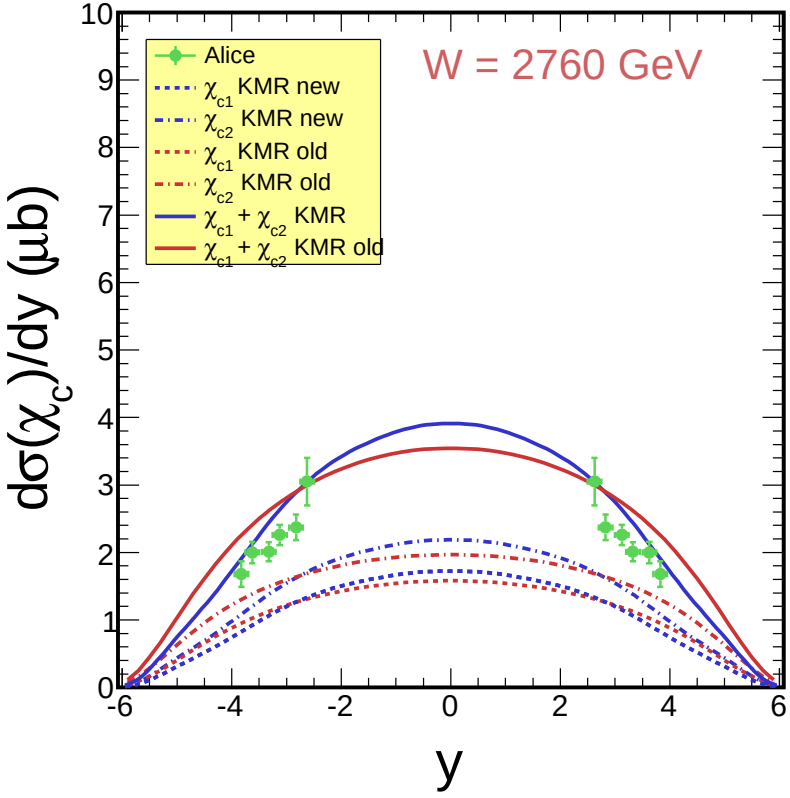

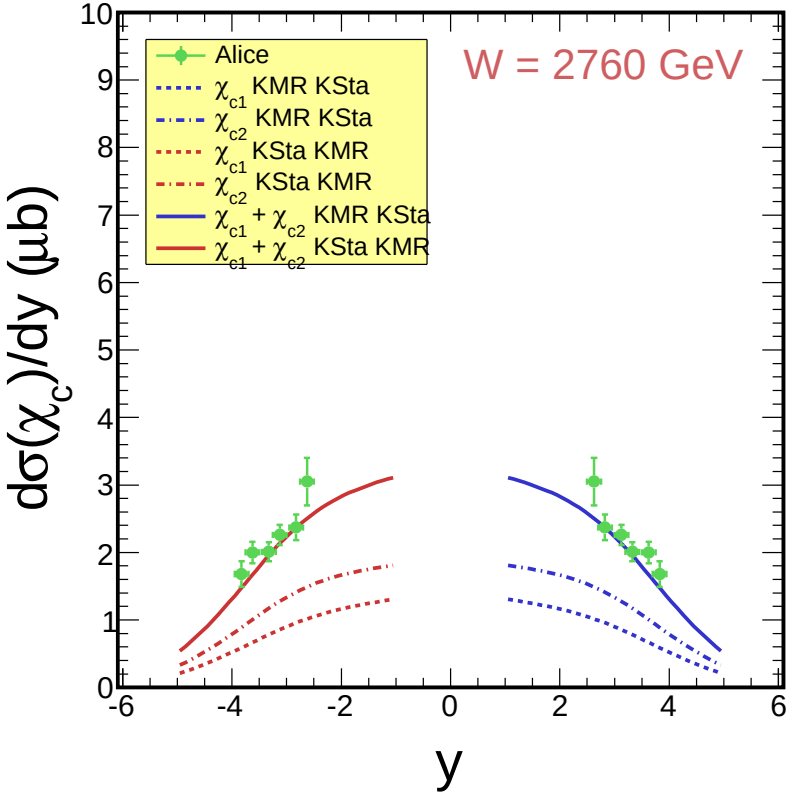

Both KMR and nonlinear KS acceptable

χ_c contribution to inclusive J/ψ

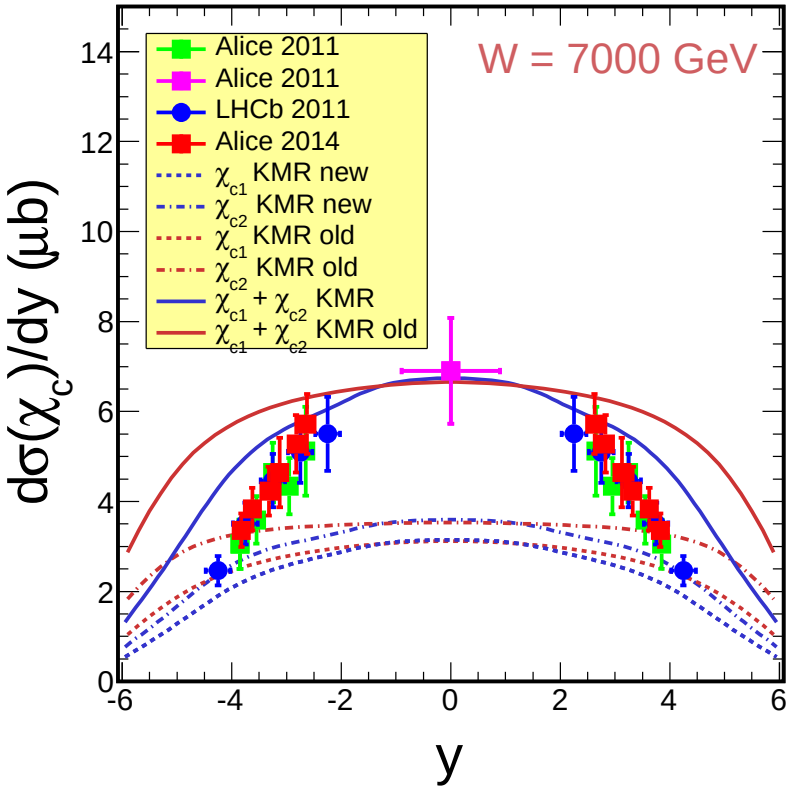

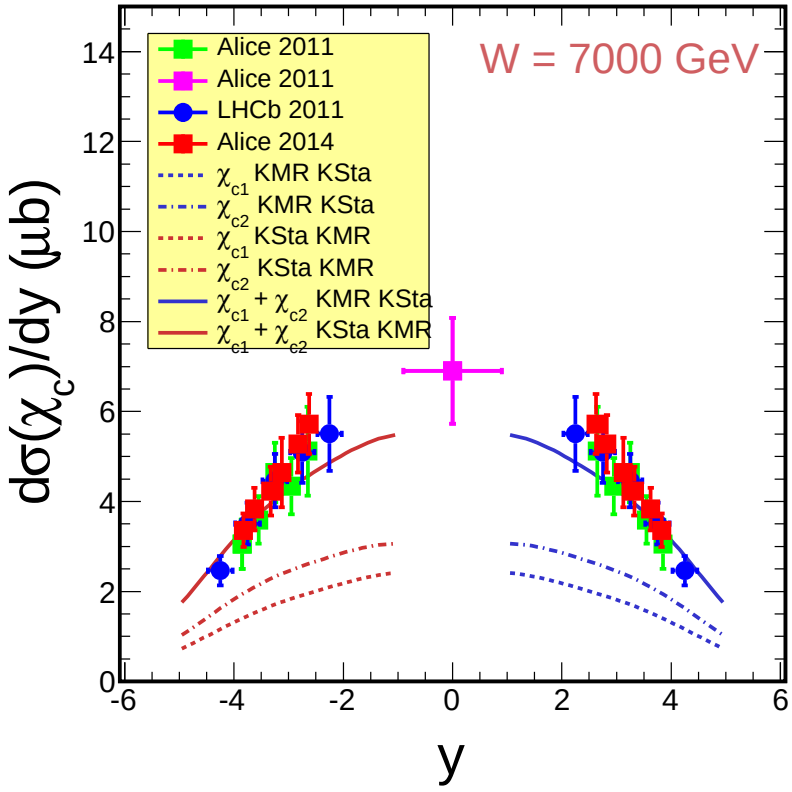

Only nonlinear KS acceptable

χ_c contribution to inclusive J/ψ

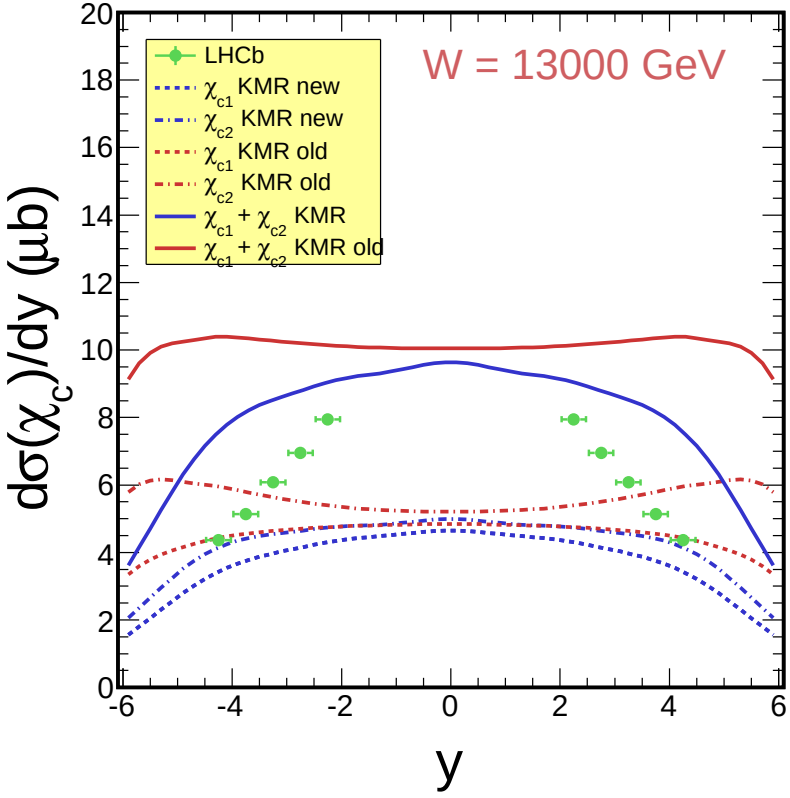

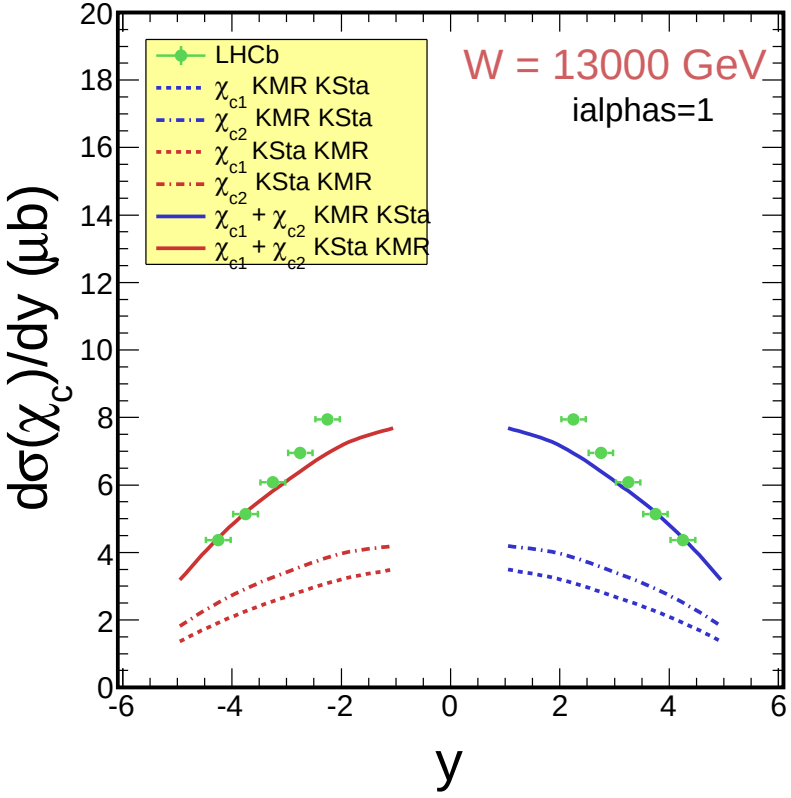

Only nonlinear KS acceptable

Conclusions, Drell-Yan

- Forward production of low-mass dileptons has been discussed
- Correponding momentum space formula has been derived and presented
- In contrast to the dipole formalism correct treatment of kinematics
  and can be applied to the analysis of real experiment
- We have obtained four terms instead of two terms in the traditional dipole approach.
- A program which includes $2 \to 3$ subprocesses has been written.
  Correlation between a jet and leptons can be calculated
- Calculation of differential cross section for experimental conditions have been performed.
- General tendencies have been shown.
- The results have been compared with LHCb and ATLAS data.
- Critical remarks to dipole model applications have been made

Conclusions, Drell-Yan

- The saturation inspired UGDFs fail to describe LHCb and ATLAS data
- KMR UGDF (relation to DGLAP approach) is much better
- Some strenght at large M_{ll} is missing (lack of meson cloud)
- Both side contributions have to be included (even for LHCb) in contrast to calculations in dipole model in the literature
- Contribution of different terms (L, T, etc) strongly depends on kinematics
- New interference terms rather small
- Meson cloud effects missing here as well as in dipole approach
- No clear hints of saturation at small M_{ll}

Conclusion, $pp \to ppJ/\psi$

There is some model dependent indication of nonlinear effects
Open problems:

- The present experiments are not exclusive.
- So far proton dissociation "extracted" in a model dependent way assuming some functional form in p_t.
- We have now better knowledge about diffractive dissociation (HERA).
- Compared to HERA there is also photon dissociation
  The contribution of electromagnetic dissociation bigger than that for diffractive dissociations.
- Interference effects due to the two diagrams were predicted. It would be nice to see modulation in ϕ_{pp} due to interference effects between the two contributing diagrams.
- CMS+TOTEM and ATLAS+ALFA could measure purely exclusive reaction and study dependences on many more variables.

Conclusion, inclusive production of J/ψ

- There seems to be a signiture of saturation at large energies (13 TeV) and large rapidities.
  Already χ_c component seems to be in conflict with the LHCb data. For comparison at low energies (2.76 GeV) more standard approach agrees with the data.
- More detailed studies are necessary to draw definite conclusions.

Conclusion, inclusive production of J/ψ

- There seems to be a signiture of saturation at large energies (13 TeV) and large rapidities.
  Already χ_c component seems to be in conflict with the LHCb data. For comparison at low energies (2.76 GeV) more standard approach agrees with the data.
- More detailed studies are necessary to draw definite conclusions.

Thank You